AD NUMBER

AD812006

NEW LIMITATION CHANGE

TO

Approved for public release, distribution unlimited

FROM

Distribution authorized to U.S. Gov't. agencies and their contractors; Critical Technology; MAR 1967. Other requests shall be referred to Air Force Weapons Lab., Kirtland AFB, NM.

AUTHORITY

AFWL ltr, 30 Nov 1971

OPACITY OF LOW-TEMPERATURE AIR

J. C. Camm
B. Kivel
R. L. Taylor
et al.

AVCO Everett Research Laboratory
A Division of AVCO Corporation
Everett, Massachusetts 02149
Contract AF 29(601)-7055

TECHNICAL REPORT NO. AFWL-TR-66-127
March 1967

AIR FORCE WEAPONS LABORATORY
Research and Technology Division
Air Force Systems Command
Kirtland Air Force Base
New Mexico

AFWL-TR-66-127

Research and Technology Division
AIR FORCE WEAPONS LABORATORY
Air Force Systems Command
Kirtland Air Force Base
New Mexico

OPACITY OF LOW-TEMPERATURE AIR

J. C. Camm
B. Kivel
R. L. Taylor
et al.
AVCO Everett Research Laboratory
A Division of AVCO Corporation
Everett, Massachusetts 02149
Contract AF 29(601)-7055

TECHNICAL REPORT NO. AFWL-TR-66-127

FOREWORD

This report was prepared by the AVCO Everett Research Laboratory (AERL), Everett, Massachusetts, under Contract AF 29(601)-7055. The research was performed under Program Element 6.16.46.01D, Project 5710, Subtask 07.003, and was funded by the Defense Atomic Support Agency (DASA).

Inclusive dates of research were 1 September 1965 to 1 September 1966. The report was submitted 8 March 1967 by the Air Force Weapons Laboratory Project Officer, Lt George E. DeBorde III (WLRT).

The contractor's report number is AERL Final Report-October 1966.

Publication of this report does not constitute Air Force approval of the report's findings or conclusions. It is published only for the exchange and stimulation of ideas.

George E. DeBorde III

GEORGE E. DeBORDE III
Lt, USAF
Project Officer

George R. Spillman, Major USAF

for RALPH H. PENNINGTON
Colonel, USAF
Chief, Theoretical Branch

CLAUDE K. STAMBAUGH
Colonel, USAF
Chief, Research Division

ABSTRACT

(Distribution Limitation Statement No. 2)

Predictions are given for the Bremsstrahlung absorption cross section of atomic oxygen and atomic nitrogen. The electron-atom interaction potential energy is adjusted to give agreement with the photo-absorption measurements of the negative oxygen ion. The exchange force is treated in an approximate manner following a suggestion by Slater but adjusted to take account of the dependence on the configuration of the electron wave. The difference in the exchange force for s- and p-waves as well as the difference between the triplet and quintet configurations in atomic nitrogen must be preserved to obtain predictions for the Bremsstrahlung which are in agreement with experiments. The atomic oxygen absorption cross section is about a factor of 5 less than that of atomic nitrogen in agreement with the measurements of Taylor. The Maxwell average atomic nitrogen Bremsstrahlung absorption cross section is insensitive to temperature. The atomic nitrogen cross section deviates somewhat from the Kramers' wavelength dependence, becoming relatively larger in the blue. The partial wave analysis for Bremsstrahlung and elastic scattering by molecular nitrogen is reviewed. These studies suggest that the Bremsstrahlung in the field of molecular nitrogen can be estimated from the measured momentum transfer cross section. Using this approximation for the molecular components and recent calculations of Bremsstrahlung in the field of atomic oxygen and nitrogen, the emissivity and intensity from neutral Bremsstrahlung in high-temperature air is estimated. A spectrometer which scans a wavelength band of 0.6 microns in 30 microseconds and is useful from 2 to 6 microns is described. Using this instrument, data have been obtained of the absolute spectral radiation intensity of air, nitrogen, neon, and argon heated by reflected shocks in shock tubes to equilibrium temperatures in the range of 6000 to 10,000°K. In this temperature regime, an important source of continuum radiation in these gases is neutral Bremsstrahlung caused by the inelastic scattering of electrons from neutral atoms and molecules.

CONTENTS

ILLUSTRATIONS

TABLES

SECTION I

NEUTRAL ATOM BREMSSTRAHLUNG

1. Introduction

In air at 8000° Kelvin and one atmosphere of density, the Bremsstrahlung from electrons accelerated in the fields of neutral atoms and molecules contributes about 10 percent of the total (spectrally integrated) emissivity. In the infrared beyond one micron, it is the major source of radiation. In early analyses of air radiation,[1, 2, 3] it was assumed for simplicity that atomic oxygen was the major source of the Bremsstrahlung, since it had the highest electron affinity. Measurements in the infrared by Wentink[4] were used to set the intensity of the neutral Bremsstrahlung. More recent and more extensive studies of the infrared radiation from air and nitrogen by Taylor[5] have demonstrated that atomic oxygen is a minor component in the Bremsstrahlung; that the radiation from air should be attributed to molecular and atomic nitrogen; and that molecular nitrogen is larger with about twice the cross section of atomic nitrogen. Since molecular nitrogen is twice as effective as atomic nitrogen, the total absorption by Bremsstrahlung is insensitive to the degree of dissociation of nitrogen. Taylor also found that the spectral distribution did not fit the simple Kramers' model. Thus the spectral extrapolation into the visible could not be reliably made. In this report, the Bremsstrahlung from neutral atomic oxygen and nitrogen on a semi-empirical basis is estimated, that is, so that it agrees with existing experimental data, and then used in the calculations to predict the spectral intensity in regions where measurements have not yet been made.

Since the early calculations of air radiation were made, there have been a number of pertinent experiments on the scattering of low-energy electrons by atomic oxygen and nitrogen. The most significant of these are the actual Bremsstrahlung measurements by Taylor, which give the ratio of contributions by molecular nitrogen, atomic nitrogen, and atomic oxygen in the infrared at 4 microns and also give the spectral intensity dependence between 4 and 2 microns. During this period, Klein and Brueckner[6] have

shown how to analyze the total absorption cross section of the negative oxygen ion measured by Branscomb[7] in terms of the low energy oxygen scattering cross section. Low energy oxygen conductivity measurements by Lin[8] are shown to be consistent with the Branscomb measurements, using the Klein and Brueckner analysis. Experiments by Alpher and White[9] which give the polarizability of atomic oxygen and nitrogen fix the long range interaction between the neutral atoms and electrons. At higher energies than of interest (5 ev and above), Neynaber[10] has measured the scattering cross section of atomic oxygen and nitrogen. These experiments constrain the theoretical model and will be used in Part 4.

In Part 2, our methods of calculation will be outlined. Here the spherically symmetric potentials are defined, which will be used in the numerical integration of the Schrödinger equation to obtain the electron wave functions and the scattering cross sections. These wave functions are used in the acceleration matrix element to determine the Bremsstrahlung. The dependence of the exchange force on the configuration is discussed in Parts 3 and 4. The potential has a polarization cut-off parameter that is fixed to agree with experimental data (Part 5). Part 6 gives results for the Bremsstrahlung absorption cross section of atomic oxygen and atomic nitrogen. Comparison is made with the measurements of Taylor. The results and uncertainties are reviewed in Part 7.

The programming of the differential equation for this Section was done by Richard Johnson and that for the absorption matrix element by Tom Tsika. Dr. Derek Teare has provided the insight and guidance required to obtain the desired numerical accuracy. The author is also indebted to Professors Henry Margenau and Hans Bethe for advice and guidance in preparing Section I.

2. Calculation Methods

A. Basic Equations

In this section the methods used to determine 1) the free electron wave function, 2) the scattering cross section, and 3) the Bremsstrahlung absorption cross section, are given.

To determine the wave functions a spherically symmetric potential (V(r)) has been assumed so that only the one-dimensional Schrödinger equations[11] need be solved. This equation is

$$\frac{d^2}{dr^2} G_\ell - \left[\frac{\ell(\ell+1)}{r^2}\right] G_\ell - 2V G_\ell = -\kappa^2 G_\ell \qquad (1)$$

The potential consists of three parts: the Coulomb interaction of the electron with the atomic electrons and nucleus. The [illegible] distribution of the bound electrons (ρ) is determined from Hartree-Fock calculations of the unperturbed atom.

$$V_{Coul.} = -\frac{Z}{r} + \frac{1}{r} \int_0^r \rho dr' + \int_r^\infty \frac{\rho}{r'} dr' \qquad (2)$$

Extending a method introduced by Slater[12] for treating the exchange force in solids, the exchange potential can be taken proportional to the local charge density to the 1/3 power

$$V_{Ex} = -\frac{\gamma}{2} \left(\frac{3}{32\pi^2} \frac{\rho}{r^2}\right)^{1/3} \propto \left(\frac{\rho}{r^2}\right)^{1/3} \qquad (3)$$

The factor which normalizes the magnitude of the potential (γ) is found by matching results with the correct atomic oxygen scattering calculation carried out for zero energy electrons with $\ell = 0$ by Bates and Massey.[13] For other states, γ is obtained by a perturbation scheme described below. The polarization force is taken account of by the term

$$V_{Pol} = -p/2 \left(r^2 + d^2\right)^2 \qquad (4)$$

For polarizability (p), the measurements of Alpher and White are used, which give for oxygen p = 5.2 and for nitrogen p = 7.6. This leaves

one free parameter d^2, which will be investigated (Part 5).

To determine the atomic charge density ρ, the results of D. R. Hartree, W. Hartree and B. Swirles[14] for oxygen and of D. R. Hartree and W. Hartree[15] for nitrogen are used. The integral from 0 to 10 of ρ is normalized to 7 for nitrogen and for oxygen to 8.

The Bremsstrahlung absorption cross section is determined by[11]

$$Q_a = \frac{256}{3}^2 \left(\frac{1}{137}\right)\left(0.529 \times 10^{-8}\right)^5 \left(\frac{M^2}{\kappa_i^2\ \kappa_f}\right)\left(\frac{1}{\Delta\kappa^2}\right)^3 \quad (5)$$

where the matrix element is

$$M^2 = \left| \int_0^\infty G_0(\kappa_i)\, G_1(\kappa_f)\ \frac{dV}{dr}\ dr \right|^2 + \left| \int_0^\infty G_0(\kappa_f)\, G_1(\kappa_i)\ \frac{dV}{dr}\ dr \right|^2 \quad (6)$$

In this matrix elementary wave functions are normalized so that their asymptotic magnitude is unity.

$$G \sim \sin\left(\kappa r - \frac{\ell\pi}{2} + \delta_\ell\right) \quad (7)$$

The matrix elements were calculated numerically both in the form given above and also in the form which is obtained by integrating by parts:

$$\left| \int \left[G_0(\kappa_i)\, G_1'(\kappa_f) + G_0'(\kappa_i)\, G_1(\kappa_f) \right] V(r)\, dr \right|^2 \quad (8)$$

This allows our results to be checked, which is important because the integral has a small final value which results from the cancellation of large positive and negative contributions.

Also programmed were a number of integrals over the exchange and polarization parts of the potential to be used in perturbation schemes to obtain the effect on the cross sections of small changes in the parameters γ, p and d^2. In terms of these integrals, corrected values of the logarithmic derivative of the wave function at the outside edge of the atom is obtained in the form, e.g.,

$$\left.\frac{G'}{G}\right)_r = \left.\frac{F'}{F}\right)_r + \frac{1}{F_r^2}\left(\int_0^r F^2 \frac{p}{(r^2+d_1^2)^2}\,dr - \int_0^r F^2 \frac{p}{(r^2+d_2^2)^2}\,dr\right) \tag{9}$$

These equations have been solved using numerical methods on an IBM computer. The Runge-Kutta method was used for solving the differential equation and a Simpson rule integration for the matrix element. Quadratic interpolation has been used for obtaining intermediate values of V and G in the integration. The differential equation was solved with a variable interval size determined so that the change in G_0 and G_1 should be on the order of 0.06 percent of its value, the change in $dG_0/dr \sim 0.3$ percent and the change in $dG_1/dr \sim 0.03$ percent. In no case was the interval size allowed to be larger than 0.05 atomic units.

B. Exchange Parameter

The exchange parameter, γ, is chosen so that

$$\int_0^\infty G_\ell^2 \, V_{Ex} \, dr = \int_0^\infty \frac{G_\ell Q_\ell}{r} \, dr \tag{10}$$

where

$$Q_\ell = \Sigma_k \Sigma_j \, b_{j,k} \, Y_k(j,\ell) \, P_j \tag{11}$$

with

$$Y_k(\alpha,\beta) = \frac{1}{r^k} \int_0^r P_\alpha P_\beta \, r'^k \, dr' + r^{k+1} \int_r^\infty P_\alpha P_\beta \, \frac{1}{r'^{k+1}} \, dr' \quad (12)$$

and P_α are the radial functions for the bound electrons. The coefficients, $b_{j,k'}$ are given by Slater.[16]

C. Quadrupole Moment

For the p orbital in the ^4P configuration, an additional energy term appears from the quadrupole moment

$$-\frac{2}{10} \, F_2$$

where

$$F_2 = \int_0^\infty G_\ell^2 \, \Delta V dr \quad (13)$$

with

$$\Delta V = \frac{2}{r^3} \int_0^r P_{2p}^2 \, r'^2 \, dr' + 2r^2 \int_r^\infty P_{2p}^2 \, \frac{1}{r'^3} \, dr' \quad (14)$$

In order to introduce the effect of this force the exchange force parameter γ is increased by an amount $\Delta\gamma$ such that

$$\frac{\Delta\gamma}{\gamma} \int G^2 \, V_{Ex} \, dr = \frac{1}{10} \, F_2 \quad (15)$$

D. Momentum and Acceleration Matrix Elements

When a different potential energy curve for the electron in an s state and for one in a p state is used, the question arises as to which of these should be used in the acceleration matrix calculation. It is noted that this problem will not arise if the momentum matrix element is used to calculate the radiation. It is therefore possible to transfer from the momentum form to the acceleration form in order to find the appropriate potential for the acceleration matrix.

The acceleration matrix to the momentum form in the case where the same potential is used for both s and p states is the starting point. By starting with the acceleration matrix and integrating by parts, the following is obtained:

$$\int \nabla V \, \psi_1 \psi_2 d\tau = -\int V(\psi_2 \nabla \psi_1 + \psi_1 \nabla \psi_2) d\tau \tag{16}$$

The following integral is then added, which is zero

$$\int (\Delta \psi_2 \nabla \psi_1 + \Delta \psi_1 \nabla \psi_2) \, d\tau \tag{17}$$

so that the acceleration matrix becomes

$$\int \nabla V \psi_1 \psi_2 \, d\tau = -\kappa_2^2 \int \psi_2 \nabla \psi_1 \, d\tau - \kappa_1^2 \int \psi_1 \nabla \psi_2 \, d\tau = (\kappa_2^2 - \kappa_1^2) \int \psi_1 \nabla \psi_2 \, d\tau \tag{18}$$

where the first term has been integrated by parts to obtain the final form. The momentum matrix element has thus been transformed which is independent of V.

If the procedure is now inverted and going from the momentum form in the case where the potential used for the two states is not the same, the following is obtained:

$$(\kappa_2^2 - \kappa_1^2) \int \psi_1 \nabla \psi_2 \, d\tau = - \int (V_2 \psi_2 \nabla \psi_1 + V_1 \psi_1 \nabla \psi_2) d\tau \qquad (19)$$

The following form is therefore used

$$\int_0^\infty \left(V_2 G_2 \frac{dG_1}{dr} + V_1 G_1 \frac{dG_2}{dr} \right) dr \qquad (20)$$

in the calculation of the acceleration matrix when different potentials are used for the s and p waves.

3. The Slater Coefficients and the Exchange Force

The Hartree-Fock method of calculating the wave function of an electron in an atom has been extended by Bates and Massey[13] to calculate the free electron s-wave for scattering by atomic oxygen. The method has been extended by Seaton[17] to treat the atomic oxygen free electron p-wave. Seaton's paper gives the details of the derivation of this method. The basic equation to be solved is

$$\left\{ \frac{d^2}{dr^2} + V + v_p + \kappa^2 - \frac{\ell(\ell+1)}{r^2} \right\} P_\ell = - \frac{2Q}{r} + \eta_{1s} P_{1s} + \eta_{2s} P_{2s} \qquad (21)$$

where

$$V = \frac{2Z}{r} - \frac{2}{r} \left\{ 2Y_o(1s, 1s) + 2Y_o(2s, 2s) + nY_o(2p, 2p) \right\} - \frac{2}{r} R$$

For nitrogen $Z = 7$ and $n = 3$; for oxygen $Z = 8$ and $n = 4$.

$$R = \sum_{k \geq 1} \sum_{j} a_{jk} \; Y_k(j, j)$$

$$Q = \sum_{k} \sum_{j} b_{jk} \; P_j \quad Y_k(j, \ell)$$

$$Y_k(\alpha, \beta) = \frac{1}{r^k} \int_0^r P_\alpha \, P_\beta \; r'^k \, dr' + r^{k+1} \int_r^\infty P_\alpha \, P_\beta \; \frac{1}{(r')^{k+1}} \, dr'$$

$$v_p = p/(r^2 + d^2)^2$$

The j sum is over the bound quantum states. The $a_{jk = 0}$ have been separated since these coefficients do not change.

The coefficients a_{jk} and b_{jk} are derived by Slater[16] for L-S coupling. The application of this method to the free p-wave of atomic oxygen is not obvious, consequently the details are given here. However, the very clear exposition given by Slater will not be repeated. In order to make the discussion easier to follow, the simpler case of a free s-wave and atomic nitrogen will be the starting point.

The state with spin projection $M_S = 2$ and angular momentum $L = 0$ is first enumerated given the coefficients for the ^5S state. The matrix for the atomic state is represented

$$\psi_{0,\, 3/2} = (1\alpha) \; (0\alpha) \; (-1\alpha) \tag{22}$$

where each parenthetical term represents an electron state. The number in the parentheses gives the angular momentum of the electron state and the Greek symbol gives its spin (α is spin up and β is spin down).

The ^5S state of atom and free s-wave is given by

$$\psi_{0,3/2}(0a)_f \tag{23}$$

where the subscript f on the last electron state indicates that it is the free electron state. For this configuration the electron energy can be determined at once from Slater's table for the coefficients a and b:

$$\underline{2F_0(1s;fs) + 2F_0(2s;fs) + 3F_0(2p;fs) - G_0(1s;fs) - G_0(2s;fs) - G_1(2p;fs)} \tag{24}$$

where

$$F^k(n\ell;n'\ell') = e^2(4\pi)^2 \int_0^\infty \int_0^\infty R^2(n\ell/r)\, R^2(n'\ell'/r')\, \frac{r_a^k}{r_b^{k+1}}\, r^2 r'^2\, dr\, dr'$$

$$G^k(n\ell;n'\ell') = e^2(4\pi)^2 \int_0^\infty \int_0^\infty R(n\ell/r)\, R(n'\ell'/r)\, R(n\ell/r')\, R(n'\ell'/r')\, \frac{r_a^k}{r_b^{k+1}} \times r^2 r'^2\, dr\, dr'$$

where those terms which are common to ^5S and ^3S have been underlined.

According to Slater's method, the two states which compose the ^3S and ^5S states are now required. These are obtained using the spin lowering operator (S^{-1}). This immediately gives the two required states as

$$(S^{-1}\ \psi_{0,3/2})\ (0\,a)_f \tag{25}$$

$$\psi_{0,3/2}\,(0\beta)_f \tag{26}$$

where

$$S^{-1}\,\psi_{0,3/2} = \frac{1}{\sqrt{3}}\left[(1\beta)\,(0\alpha)\,(-1\alpha) + (1\alpha)\,(0\beta)\,(-1\alpha) + (1\alpha)\,(0\alpha)\,(-1\beta)\right] \tag{27}$$

where each of the terms in the square brace are matrices for three electron states. With these wave funtions, the energy can be evaluated via Slater's method. It should be noted that the cross terms which result because the atomic state has three terms, do not contribute anything because of orthogonality properties, i.e., the interaction potential involves two electrons, one of which is in the free state but the terms in the atomic state differ by two electron states so that one of these will be orthogonal upon integrating. A value of one-third the sum of the contributions of each individual term is obtained; so that the energy for $^5S + {}^3S$, in addition, to twice the common energy terms underlined above has the value for the 2p-fs interaction

$$-\frac{2}{3}\,G_1\,(2p;fs) \tag{28}$$

Subtracting the energy of ^5S yields the energy for ^3S, which, in addition to the common underlined terms in Eq (4), gives

$$+\frac{1}{3}\,G_1\,(2p;fs) \tag{29}$$

The methods for the nitrogen free p-wave and the oxygen free s-wave are similar and only the results will be given in these cases. The common terms for the nitrogen ^5P and ^3P are

$$2F_0(1s;fp) + 2F_0(2s;fp) + 3F_0(2p;fp) - \frac{1}{3}\,G_1(1s;fp) - \frac{1}{3}\,G_1(2s;fp) \tag{30}$$

The 2p-fp interaction terms for ^5P is

$$-G_0(2p;fp) - \frac{10}{25} G_2(2p;fp) \tag{31}$$

and for the ^3P

$$+ \frac{1}{3} G_0 (2p;fp) + \frac{10}{75} G_2(2p;fp) \tag{32}$$

For atomic oxygen plus a free s-wave the terms common to ^4P and ^2P are

$$2F_0(1s,4s) + 2F_0(2s;fs) + 4F_0(2p;fs) - G_0(1s;fs) - G_0(2s;fs) \tag{33}$$

The 2p-fs interaction for ^4P is

$$-G_1 (2p;fs) \tag{34}$$

and for ^2P it is zero.

The states for a free p electron and atomic oxygen are more complex. It is desirable to have the energy of the six states of the doublets S, P and D and the quartets S, P and D are desired. These are found by evaluating the energy of six states which are enumerated below and taking the differences. In order to find the appropriate wave functions to determine these energies, the angle of momentum lowering operator (L^{-1}) in addition to the spin lowering operator is introduced. The wave function for the ground state of the atom will be abbreviated as

$$\psi_{1,1} = (1\alpha)\,(0\alpha)\,(-1\alpha)\,(1\beta) \tag{35}$$

In applying the lowering operators to this function, it is important to remember that the functions indicated as a product are in fact a matrix so that an interchange of two states is the same as interchanging two columns of the matrix, which changes the sign of that term. There are two things which prevent lowering a state. One is the Pauli exclusion principle so that, for example, the 1α state cannot be lowered to 1β when an electron is already

in the 1β state. The other occurs when the state has the lowest quantum value, e. g., the β state cannot be lowered further. The lowering operator is the sum of operators which lower each state separately. In Table I the wave functions for the six appropriate combined states are given. Table II gives the atomic part of the wave functions (again, these are abbreviated in product form, each product representing a 4-electron matrix). The common energy terms are

$$2F_0(1s;fp) + 2F_0(2s;fp) + 4F_0(2p;fp) - \tfrac{1}{3} G_1(1s;fp) - \tfrac{1}{3} G_1(2s;fp).$$

The additional terms which depend on the configuration are given in Table III.

The integrals required for evaluating the exchange force according to the Hartree-Fock method have been programmed, so that it is now possible to determine an effective value for the exchange force parameter γ such that the integral of the exchange force times the square of the wave function will equal the integral of the wave function times the corresponding quantity in the Hartree-Fock equation (2QG/r).

$$\frac{\gamma'}{\gamma} \int_0^\infty V_{exch} G^2 dr = \int \frac{2QG}{r} dr \qquad (36)$$

The values used for the coefficients $b_{j,k}$ and the estimated values of γ are given in Table IV. In determining γ solutions of Eq. (1) where $\gamma = 1.3$, $p = 5.2$, $d^2 = 1.97$, and $\kappa = 0.2$ for oxygen and $\gamma = 1.3$, $p = 7.6$, $d^2 = 2.30$ and $\kappa = 0.2$ for nitrogen were used. At zero energy, the value for the average configuration for oxygen for $\ell = 0$ approaches $\gamma = 1.3$, which gives the same scattering length as the calculation of Bates and Massey. This indicates that the approximate method has validity and in particular is good for the s-waves.

The γ are not independent of the electron energy; however, they will be treated as constants. The results in Table V indicate the variation of γ with energy.

TABLE I

States for Oxygen (^3P) Plus Free p

Configurations	Wave Functions
^4D	$\psi_{1,1}\,(1\alpha)_f$
$^2D + {}^4D$	$(S^{-1}\psi_{1,1})\,(1\alpha)_f$
	$\psi_{1,1}\,(1\beta)_f$
$^4D + {}^4P$	$(L^{-1}\psi_{1,1})\,(1\alpha)_f$
	$(\psi_{1,1})\,(0\alpha)_f$
$^4D + {}^4P + {}^4S$	$(L^{-2}\psi_{1,1})\,(1\alpha)_f$
	$(L^{-1}\psi_{1,1})\,(0\alpha)_f$
	$\psi_{1,1}\,(-1\alpha)_f$
$^2D + {}^2P + {}^4D + {}^4P$	$(L^{-1}S^{-1}\psi_{1,1})\,(1\alpha)_f$
	$(S^{-1}\psi_{1,1})\,(0\alpha)_f$
	$(L^{-1}\psi_{1,1})\,(1\beta)_f$
	$\psi_{1,1}\,(0\beta)_f$
$^2D + {}^2P + {}^2S + {}^4D + {}^4P + {}^4S$	$(S^{-1}L^{-2}\psi_{1,1})\,(1\alpha)_f$
	$(L^{-2}\psi_{1,1})\,(1\beta)_f$
	$(S^{-1}L^{-1}\psi_{1,1})\,(0\alpha)_f$
	$(L^{-1}\psi_{1,1})\,(0\beta)_f$
	$(S^{-1}\psi_{1,1})\,(-1\alpha)_f$
	$\psi_{1,1}\,(-1\beta)_f$

TABLE II

Wave Function Gas Ground State of Atoms

$$\psi_{1,1} = (1\alpha)\,(0\alpha)\,(-1\alpha)\,(1\beta)$$

$$S^{-1}\psi_{1,1} = \frac{1}{\sqrt{2}}\left[(1\alpha)\,(0\beta)\,(-1\alpha)\,(1\beta) + (1\alpha)\,(0\alpha)\,(-1\beta)\,(1\beta)\right]$$

$$L^{-1}\psi_{1,1} = (1\alpha)\,(0\alpha)\,(-1\alpha)\,(0\beta)$$

$$L^{-2}\psi_{1,1} = (1\alpha)\,(0\alpha)\,(-1\alpha)\,(-1\beta)$$

$$S^{-1}L^{-1}\psi_{1,1} = \frac{1}{\sqrt{2}}\left[(1\beta)\,(0\alpha)\,(-1\alpha)\,(0\beta) + (1\alpha)\,(0\alpha)\,(-1\beta)\,(0\beta)\right]$$

$$S^{-1}L^{-2}\psi_{1,1} = \frac{1}{\sqrt{2}}\left[(1\beta)\,(0\alpha)\,(-1\alpha)\,(-\beta) + (1\alpha)\,(0\beta)\,(-1\alpha)\,(-1\beta)\right]$$

TABLE III

Energy Terms That Depend on Configuration for Oxygen (^3P) Plus Free p-wave

Configuration	2p;fp Energy Terms
^4P	$- G_0 - \frac{10}{25} G_2 - \frac{5}{25} F_2$
^4D	$- G_0 - \frac{10}{25} G_2 + \frac{1}{25} F_2$
^2D	$- G_0 + \frac{3.5}{25} G_2 + \frac{1}{25} F_2$
^2S	$- G_0 - \frac{10}{25} G_2 + \frac{10}{25} F_2$
^4S	$- G_0 - \frac{10}{25} G_2 + \frac{10}{25} F_2$
^2P	$+2G_0 - \frac{2.5}{25} G_2 - \frac{5}{25} F_2$

TABLE IV

Effective Exchange Force Parameter

ℓ	config	Y	$b_{\ell m, k}$*								
			k =	0			1			2	
			ℓm =	1s	2s	2p	1s	2s	2p	1s	2s	2p
			A. Oxygen									
0	^2P	0.93		1	1							
	ave.	1.41		1	1				2/3			
	^4P	1.65		1	1				1			
1	^4P	4.67				1		1/3	1/3			$\frac{10}{25}$
	^4D	4.67				1		1/3	1/3			$\frac{10}{25}$
	ave.	3.42				2/3		1/3	1/3			$\frac{4}{15}$
	^2D	3.73				1		1/3	1/3			$-\frac{3.5}{25}$
	^2S-^4S	4.67				1		1/3	1/3			$\frac{10}{25}$
	^2P	-5.19				-2		1/3	1/3			$\frac{1}{10}$
	B. Nitrogen											
0	^3S	0.74		1	1				-1/3			
	ave.	1.40		1	1				1/2			
	^5S	1.79		1	1				1			
1	^3P	-0.29				-1/3		1/3	1/3			$-\frac{10}{75}$
	ave.	2.63				1/2		1/3	1/3			$\frac{2}{10}$
	^5P	4.39				1		1/3	1/3			$\frac{10}{25}$

*Blanks are zero. Negative signs are repulsive.

TABLE V

Dependence of γ on κ for the average force*

κ	$\gamma_{\ell = 0}$	$\gamma_{\ell = 1}$
0.1414	1.36	3.51
0.2	1.41	3.42
0.4	1.67	3.03

*See Table IV for the $b_{\ell m, k}$ used for the average configuration.

4. Use of an Average Exchange Force

A. Oxygen

In order to determine the average value, the Slater coefficients have been averaged and weighted with the degeneracy of the configuration. For example, in the $\ell = 0$ (s-wave) case for oxygen, the coefficient for the first order term coupling the free-p to the 2p wave has a coefficient of zero for the doublet P configuration and a coefficient which is one for the quartet P. The average has a coefficient of 2/3 for this term in the expression for Q.

The $\ell = 1$ effective values of γ for oxygen have a wide range of values. If the quadrupole force is included in the effective γ then the magnitude for the quartet P would be increased (~ 0.4) and the magnitude for the doublet P decreased (~ 0.4), since the quadrupole force is attractive for both of these states. The quadrupole force does not affect the average value since, in this approximation, the atom is spherically symmetric. The average value is close to those for the quartet D and doublet D, since these have the dominance in the statistical weighting.

The phase shifts for the $\ell = 1$ have been calculated for oxygen as a function of electron energy using $p = 5.2$ $d^2 = 20$. The value for γ was taken as a parameter and calculations were run for $\gamma = 0,\ 1.3,\ 3.4,\ 4.67$. The cross sections for the larger two are small throughout the energy range of interest and extending up to 1 atomic unit, indicating that these potentials put the free wave close to antiresonance. This is not true for the small γ cases; however, since these correspond to states with low statistical weight in the averaging, it will be assumed that the deviations resulting from these values of the parameter will not be important in the radiation prediction.

The $\ell = 0$ for oxygen does not have a large range of γ, and its average value will be used.

B. Nitrogen

Whether neutral atomic nitrogen Bremsstrahlung can be treated by an average potential or requires individual treatment for the triplet and

quintet configurations is considered. In order to obtain some guidance in this matter, the elastic scattering cross section for electrons with energy of 1/2 ev ($\kappa = 0.2$), has been calculated. In doing this, the effective values of the exchange force (γ) determined earlier have been used. The results are summarized in Table VI.

For $d^2 = 25$ and for the s-wave results, it is seen that the scattering cross section for triplet S, quintet S, and the average are all close to 2×10^{-15} cm^2. On the other hand, the p-wave cross section is very sensitive to the exchange parameter going from an almost antiresonance cross section for triplet S to a large value of 5.7×10^{-15}cm^2. This is not like oxygen where the important p-waves are near antiresonance and the Bremsstrahlung is insensitive to the p-wave function.

For $d^2 = 5$ the s-wave results vary, but the average γ gives a cross section close to the average cross section. This is not true for the p-wave where the average γ gives a cross section near antiresonance. Since the average γ gives a poor result for the p-waves, the atomic nitrogen Bremsstrahlung for the triplet and quintet configurations have been calculated separately and then averaged.

C. Oxygen Radiation

A series of calculations for oxygen have been carried out in which the parameter for the exchange force on the p-wave (γ_1) has been varied. The motivation for this study arises from the fact that there are six p-wave configurations (^2S, ^2P, ^2D, ^4S, ^4P, ^4D). Not only the exchange force but also the quadrupole force varies with the configuration. Since there is not a separate expression in the equation for the quadrupole potential, the various values of γ should be considered as a generalized parameter to adjust for the complete change in force with the configuration change.

The results of this study are summarized in Table VII. Values are included in which the potential is truncated at $r = 5$, as well as at $r = 10$. The values for the truncated potential correspond to a weaker force between electron and atom with a somewhat unrealistic shape. It is felt that this information, which is readily available as additional output, is useful support in understanding the trends of neutral Bremsstrahlung. It is observed

TABLE VI

Nitrogen Elastic Scattering Cross Section

$\kappa = 0.2$			$p = 7.6$		$d^2 = 25$	$r = 10$
config.	γ_0	$Q_0(cm^2)\times10^{16}$	config.	γ_1	$Q_1(cm^2)\times10^{16}$	$(Q_0+Q_1)\times10^{16}$
^3S	0.74	17.8	^3P	0	0.20	18.0
average	1.4	24.3	average	2.63	9.80	34.1
^5S	1.79	22.1	^5P	4.39	56.9	79.0

$\kappa = 0.2$			$p = 7.6$		$d^2 = 5.0$	$r = 10$
config.	γ_0	$Q_0(cm^2)\times10^{16}$	config.	γ_1	$Q_1(cm^2)\times10^{16}$	$(Q_0+Q_1)\times10^{16}$
^3S	0.74	11.1	^3P	-0.29	0.37	11.5
average	1.4	4.14	average	2.63	0.07	4.2
^5S	1.79	1.25	^5P	4.39	11.9	13.1

TABLE VII

Sensitivity to the p-wave exchange force of the elastic scattering and Bremsstrahlung.

Case	γ_1	$Q_0(cm^2)\times10^{16}$	$Q_1(cm^2)\times10^{16}$	$2.9\times10^{-19}(Q_0+Q_1)(cm^5)$	$Q_a(cm^5)$
A. Oxygen $r = 10$, $p = 5.2$, $d^2 = 20$, $\gamma_0 = 1.4$, $\kappa = .2$, $\Delta\kappa^2 = 10^{-3}$					
1	0	4.93	0.13	1.5×10^{-34}	1.3×10^{-34}
2	1.4	4.93	6.46	3.3×10^{-34}	3.9×10^{-34}
3	3.4	4.93	0.82	1.7×10^{-34}	1.9×10^{-34}
4	4.67	4.93	6.85	3.4×10^{-34}	5.5×10^{-34}
B. Oxygen, $r = 5$, $p = 5.2$, $d^2 = 20$, $\gamma_0 = 1.4$, $\kappa = .2$, $\Delta\kappa^2 = 10^{-3}$					
5	0	8.74	0.05	2.5×10^{-34}	1.9×10^{-34}
6	1.4	8.74	3.20	3.5×10^{-34}	4.5×10^{-34}
7	3.4	8.74	0.01	2.5×10^{-34}	3.8×10^{-34}
8	4.67	8.74	0.66	2.7×10^{-34}	1.3×10^{-34}

TABLE VII (continued)

Case	γ_1	$Q_0(cm^2)\times10^{16}$	$Q_1(cm^2)\times10^{16}$	$1.24\times10^{-20}(Q_0+Q_1)(cm^5)$	$Q_a(cm^5)$
C. Oxygen, $r = 10$, $p = 5.2$, $d^2 = 10$, $\gamma_0 = 1.4$, $\kappa = .14$, $\Delta\kappa^2 = 2 \times 10^{-3}$					
9	0	3.21	0.06	4.0×10^{-36}	3.9×10^{-36}
10	3.4	3.21	0.41	4.5×10^{-36}	2.0×10^{-35}
11	4.67	3.21	2.56	7.2×10^{-36}	5.4×10^{-35}
D. Oxygen, $r = 5$, $p = 5.2$, $d^2 = 10$, $\gamma_0 = 1.4$, $\kappa = .14$, $\Delta\kappa^2 = 2 \times 10^{-3}$					
12	0	8.14	0.02	1.0×10^{-35}	8.0×10^{-36}
13	3.4	8.14	0.00	1.0×10^{-35}	3.1×10^{-36}
14	4.67	8.14	0.21	1.0×10^{-35}	9.9×10^{-36}

TABLE VII (continued)

Case	γ_1	$Q_0 \times 10^{16}$	$Q_1 \times 10^{16}$	$[2.9 \times 10^{-19}(Q_0+Q_1)]\,(cm^5) \times 10^{34}$	$Q_a(cm^5) \times 10^{34}$
E. Oxygen, $r = 10$, $p = 5.2$, $d^2 = 20$, $\gamma_0 = 1.3$, $\kappa = 0.2$, $\kappa = 0.2$, $\Delta\kappa^2 = 10^{-3}$					
1	0	5.76	.131	1.7	1.53
2	.6	5.76	.753	1.9	1.71
3	1.3	5.76	4.60	3.0	3.77
4	2.0	5.76	89.6	28.	76.0
5	2.7	5.76	.082	1.7	2.49
6	3.4	5.76	.823	1.9	2.06
7	4.0	5.76	2.83	2.5	3.00
8	4.67	5.76	6.84	3.6	5.47
F. Oxygen, $r = 5$, $p = 5.2$, $d^2 = 20$, $\gamma_0 = 1.3$, $\kappa = 0.2$, $\Delta\kappa^2 = 10^{-3}$					
1	0	9.48	.055	2.7	2.09
2	.6	9.48	.310	2.8	2.32
3	1.3	9.48	2.21	3.4	4.40
4	2.0	9.48	96.5	31.	75.4
5	2.7	9.48	.79	3.0	0.81
6	3.4	9.48	.01	2.7	0.43
7	4.0	9.48	.12	2.8	0.64
8	4.67	9.48	.66	2.9	1.28

TABLE VII (continued)

Case	γ_1	$Q_0 \times 10^{16}$	$Q_1 \times 10^{16}$	$[2.9 \times 10^{-19}(Q_0+Q_1)]$ $(cm^5) \times 10^{34}$	$Q_a (cm^5) \times 10^{34}$
	G. Oxygen, $r = 10$, $p = 5.2$, $d^2 = 4.0$, $\gamma_0 = 1.3$, $\kappa = 0.14$, $\Delta\kappa^2 = 2 \times 10^{-3}$				
				$1.24 \times 10^{-20}(Q_0+Q_1)(cm^5)$	$Q_a (cm^5)$
15	3.4	1.83	.769	3.2×10^{-36}	2×10^{-35}
	H. Oxygen, $r = 5$, $p = 5.2$, $d^2 = 4.0$, $\gamma_0 = 1.3$, $\kappa = 0.14$, $\Delta\kappa^2 = 2 \times 10^{-3}$				
				$1.24 \times 10^{-20}(Q_0+Q_1)(cm^5)$	
16	3.4	6.37	.019	7.9×10^{-36}	2.5×10^{-36}

that the relation between the elastic scattering cross section and the Bremsstrahlung given by the Born approximation[18] is generally useful. There is one case (case 11, Table VII) where the Born relation gives an erroneous prediction by a factor of almost 10.

The coefficient in the relation between elastic scattering (Q) and Bremsstrahlung cross sections (Q_a) is

$$Q_a = 2.9 \times 10^{-19} \left(\frac{\kappa}{0.2}\right)^3 \left(\frac{10^{-3}}{\Delta\kappa^2}\right)^3 Q \qquad (37)$$

Another aspect of these results is sensitivity of the predicted Bremsstrahlung to the variable force on the p-wave (γ_1). Large changes in this parameter (γ_1) do not make corresponding changes in the radiation prediction. This result is explained by the large elastic scattering contribution of the s-wave so that changes in the p-wave scattering do not make large changes in the total scattering cross section. Then, insofar as the Born approximation is correct, the radiaton prediction is not sensitive to the p-wave phase shift. This is a second reason for the validity of using the average γ values for estimating the average Bremsstrahlung in oxygen.

5. Adjustment of the Potential

A. Oxygen

Klein and Bruekner[6] have shown how to analyze the photo-absorption cross section measurements of negative atomic oxygen in terms of the s-wave phase shifts. In a paper by Lin and Kivel[8] these calculations are extended and results for electron scattering lengths a = 1 and 1.6 are compared with the photo-absorption cross section measurements of Branscomb, et al.[7] A potential which gives scattering lengths in this range is sought.

For the s-wave in the doublet configuration the value $\gamma = 0.93$ is used (Table IV). The polarizability is set according to the measurements of Alpher and White[9] at p = 5.2. The polarization cut-off d^2 is adjusted to obtain agreement with the negative oxygen photo-absorption data of Branscomb et al.[7] using the method of Klein and Brueckner. For $d^2 = 4.0$, the following values are obtained for the scattering length $a = 1/\kappa \operatorname{ctn} \delta_0$:

κ	$h\nu$ (ev)	$1/\kappa \text{ctn } \delta_0$
.15	1.7	1.2
.21	2.1	1.3
.33	2.9	1.5

These values give a slope for the photo-absorption cross section vs photon energy ($h\nu$) intermediate between that illustrated in Reference 8 for scattering lengths a = 1.0 and 1.6. This is in good agreement with the data. The magnitude of the cross section is slightly below the data. The elastic scattering cross section at 1/4 ev is consistent with Lin's measurement ($\sim 2 \times 10^{-16} cm^2$) and at 5 ev with Neynaber ($\sim 6 \times 10^{-16} cm^2$). The cross section, peaks in the neighborhood of 2 ev at $Q = 8 \times 10^{-16} cm^2$ (Fig. 1).

B. Nitrogen

By scaling from oxygen[19] by taking $d^2 \propto p^{1/2} Z^{-1/6}$ the value of $d^2 = 5$ for nitrogen is obtained. Figure 2 shows the cross section for $\ell = 1$ at $\kappa = 0.2$ and 0.6 as a function of d^2. For values of d^2 less than 5 the p-wave scattering in both triplet and quintet configurations gets very large, which at $\kappa = 0.6$ would disagree with the measurements of Neynaber. On the other hand, for values of d^2 larger than 5, the s-wave cross section at $\kappa = 0.2$ becomes large which probably would lead to a contradiction with the IR Bremsstrahlung measurement of Taylor. Thus, the suggested scaling from oxygen leads to an acceptable potential for use in predicting nitrogen Bremsstrahlung. However, it is about twice the measurement of Neynaber (Fig. 3).

In order to show that the calculated cross section, which at large energy is larger than the measurements of Neynaber, is not improved by a weaker potential Table VIII is given showing the cross sections when the potential is set equal to zero beyond a cut-off radius (r_c). It can be seen

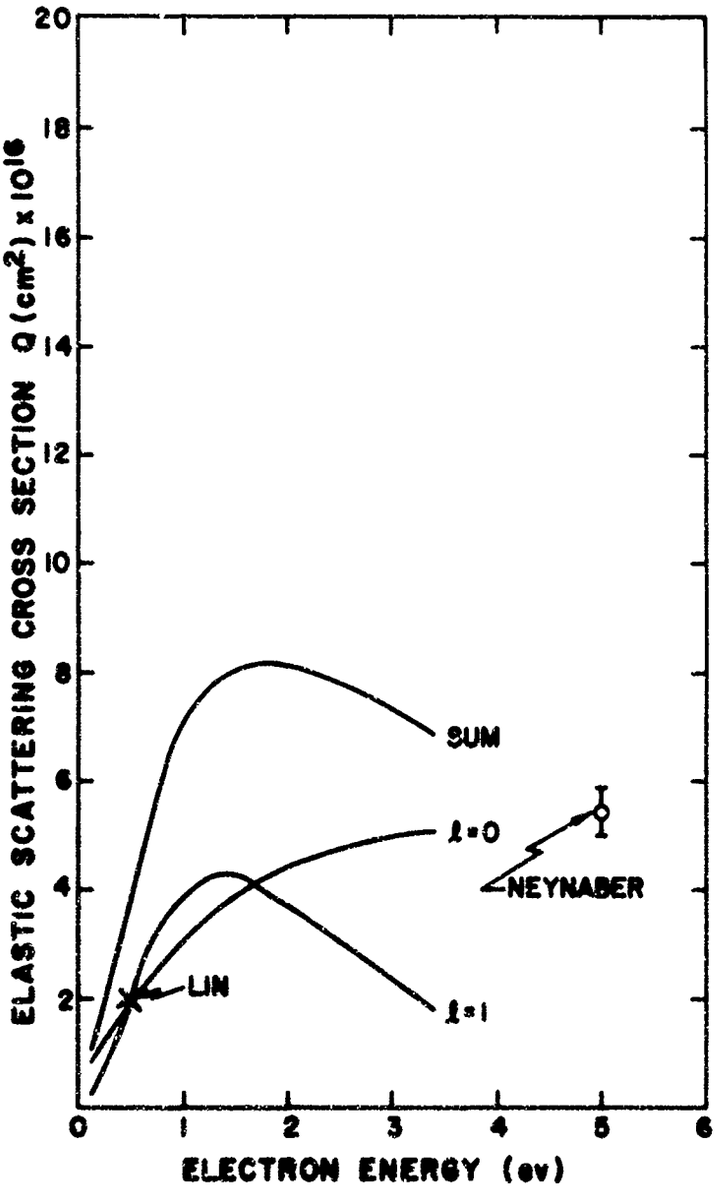

Fig. 1 Elastic scattering cross section of atomic oxygen as a function of electron energy, taking into account only the first two partial waves (ℓ = 0 and 1) for $p = 5.2$, $d^2 = 4.0$, $\gamma_0 = 1.4$ and $\gamma_1 = 3.4$.

A9707

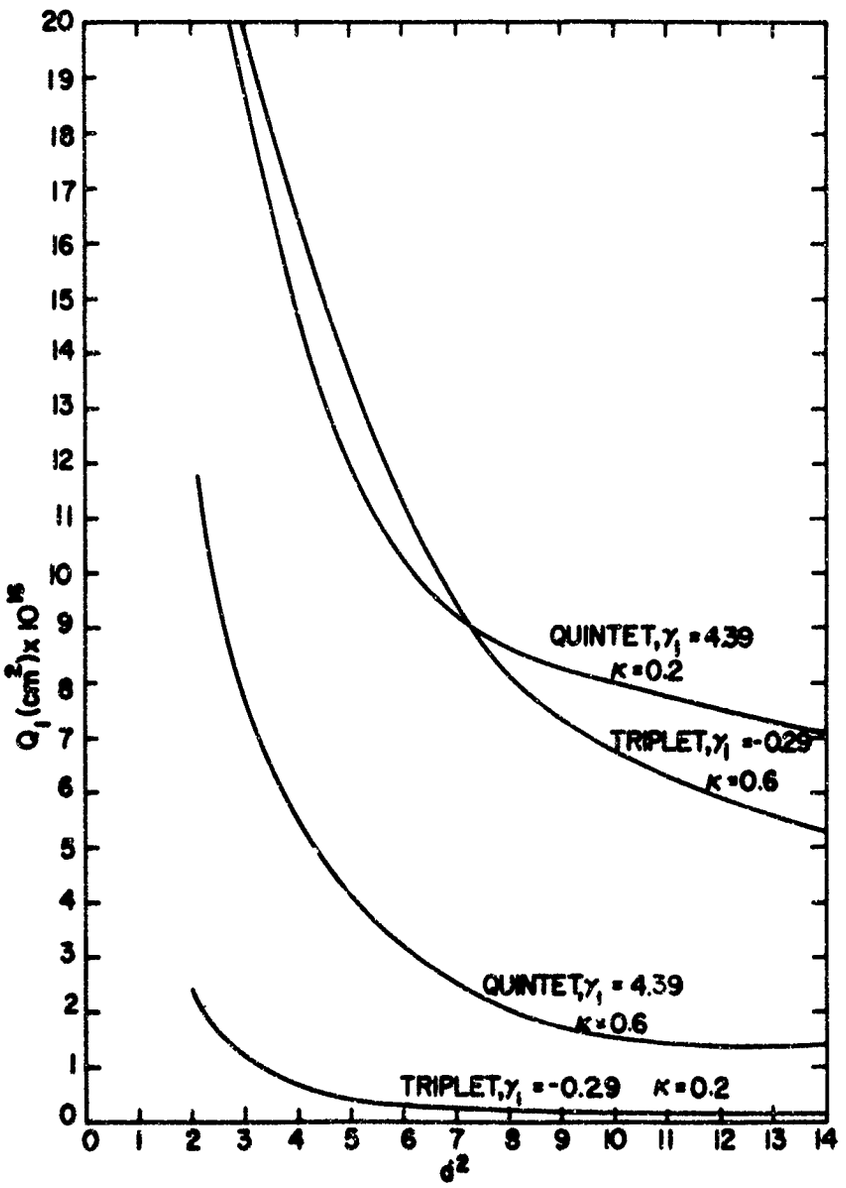

Fig. 2 The p-wave contribution to the elastic scattering cross section of atomic nitrogen as a function of the polarization cut-off parameter d^2 for the quintet and triplet configurations at electron wave number $\kappa = 0.2$ and 0.6, using a polarization constant $p = 7.6$.

A3766

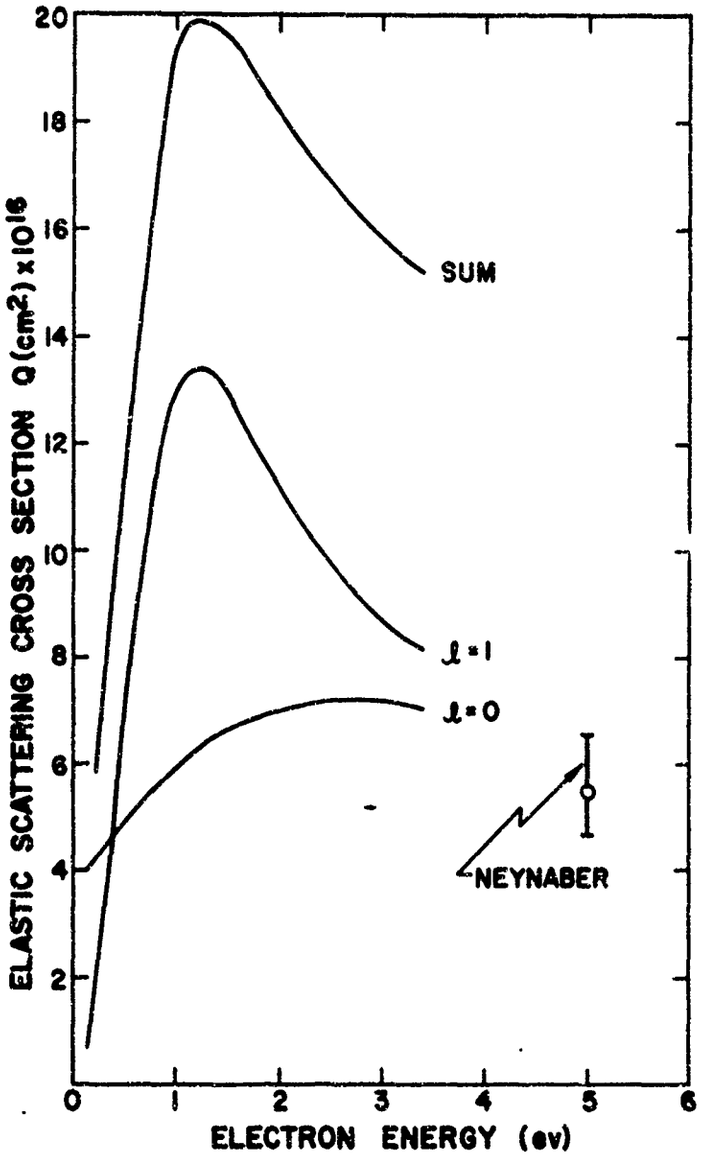

Fig. 3 Average elastic scattering cross section of atomic nitrogen as a function of electron energy, taking into account only the first two partial waves (ℓ = 0 and 1) for p = 7.6, d^2 = 5.0. Separate exchange force parameters are used for triplet and quintet scattering cross sections.

TABLE VIII

Elastic Scattering Cross Section for

N for $V = 0$ at $r > r_c$

$[Q(cm^2) \times 10^{16}]$

κ	$r_c = 5$	6	7	10
0.1	11.1	8.2	6.4	4.7
0.2	10.9	9.8	10.0	12.6
0.4	11.5	15.2	16.9	17.9
0.5	13.4	14.8	15.2	15.3

that at energy of several ev the cross section is invariably larger than Neynaber's. In addition the weaker force gives a larger cross section at low energies. It would appear that our model which fits the other available data predicts about twice the value reported by Neynaber of the elastic scattering of 5 ev electrons by nitrogen.

6. Results

The Bremsstrahlung absorption cross section for atomic oxygen is calculated using a polarizability p = 5.2 and a cut-off parameter $d^2 = 4.0$. Different exchange forces were used for the s and p-waves; i.e., $\gamma_0 = 1.4$ and $\gamma_1 = 3.4$.

The results for initial electron wave number of $\kappa_i = 0.1,\ 0.1414,\ 0.2,\ 0.2449$, are given in Fig. 4 and Table IX. These values are consistent with the measurements of Taylor[5] of the IR Bremsstrahlung. Using $Z^2 = 0.2 \times 10^{-2}$ and Kramers' interpolation, Taylor obtains

$$Q_a \doteq 4.9 \times 10^{-38} \left(\frac{\lambda}{1.2\mu}\right)^3 \left(\frac{9000^\circ K}{T}\right)^{1/2} \quad cm^5$$

Figure 4 shows Q_a for $T = 9000^\circ K$, which is consistent with the present calculations.

The results are consistent with Hundley's[18] approximation. For example, at $\kappa = 0.2$ the elastic scattering cross section is about $5 \times 10^{-16} cm^2$, which, according to Hundley, corresponds to $Q_a = 1.5 \times 10^{-37} cm^5$ at $\Delta\kappa^2 = 10^{-2}$.

The results for $\gamma_0 = 1.3$ are given in Fig. 5 and Table X. As pointed out in Table V, the γ are not strictly independent of energy. These results allow the uncertainty of the method to be indicated because of neglecting this effect.

The results for nitrogen are given in Fig. 6 and Table XI. Figure 6 contains the average over the separately calculated quintet and triplet absorption cross sections. The individual values are preserved in the table. Since the data for different initial electron energies fall essentially on the same curve, the results in this system are insensitive to electron energy

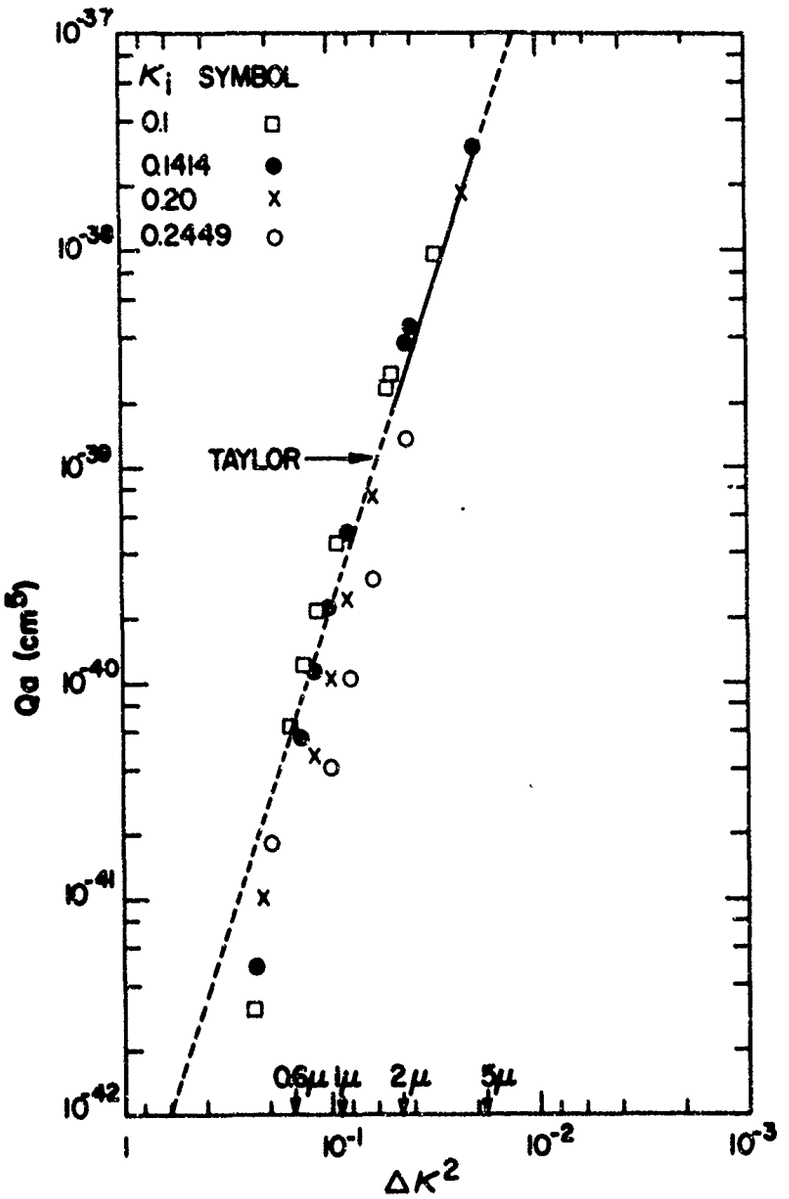

Fig. 4 Bremsstrahlung absorption cross section vs the photon energy in units of $e^2/2a$ for atomic oxygen with $p = 5.2$ and $d^2 = 4.0$. Different exchange force parameters are used for s and p-waves ($\gamma_0 = 1.4$ and $\gamma_1 = 3.4$). Values are shown for four initial wave numbers. The dashed line is an extrapolation of Taylor's measurements using $Z^2 = 0.2 \times 10^{-2}$ with T = 9000°K in the Kramers' formula.

TABLE IX

Oxygen Absorption Cross Section for $p = 5.2$, $d^2 = 4.0$, $\gamma_0 = 1.4$ and $\gamma_1 = 3.4$.

κ_i	κ_f	$Q_a(cm^5) \times 10^{40}$	κ_i	κ_f	$Q_a(cm^5) \times 10^{40}$
0.1000	0.1414	1.42E 03	0.2000	0.5000	1.02E-01
0.1000	0.2000	9.69E 01	0.2449	0.2500	9.75E 04
0.1000	0.2449	2.71E 01	0.2449	0.3194	1.34E 01
0.1000	0.2500	2.38E 01	0.2449	0.3493	3.04E 00
0.1000	0.3194	4.50E 00	0.2449	0.3742	1.04E 00
0.1000	0.3493	2.21E 00	0.2449	0 4000	4.10E-01
0.1000	0.3742	1.20E 00	0.2449	0.5000	1.84E-01
0.1000	0.4000	6.20E-01	0.2500	0.3194	1.50E 01
0.1000	0.5000	3.15E-02	0.2500	0.3493	3.14E 00
0.1414	0.2000	3.00E 02	0.2500	0.3742	1.03E 00
0.1414	0.2449	4.51E 01	0.2500	0.4000	4.01E-01
0.1414	0.2500	3.79E 01	0.2500	0.5000	1.97E-01
0.1414	0.3194	5.00E 00	0.3194	0.3493	1.00E 01
0.1414	0.3493	2.25E 00	0.3194	0.3742	8.05E-01
0.1414	0.3742	1.15E 00	0.3194	0.4000	5.68E-01
0.1414	0.4000	5.68E-01	0.3194	0.5000	5.71E-01
0.1414	0.5000	4.91E-02	0.3493	0.3742	4.77E 00
0.2000	0.2449	2.69E 02	0.3493	0.4000	2.92E 00
0.2000	0.2500	1.88E 02	0.3493	0.5000	1.02E 00
0.2000	0.3194	7.11E 00	0.3742	0.4000	3.56E 01
0.2000	0.3493	2.48E 00	0.3742	0.5000	1.81E 00
0.2000	0.3742	1.09E 00	0.4000	0.5000	3.75E 00
0.2000	0.4000	4.82E-01			

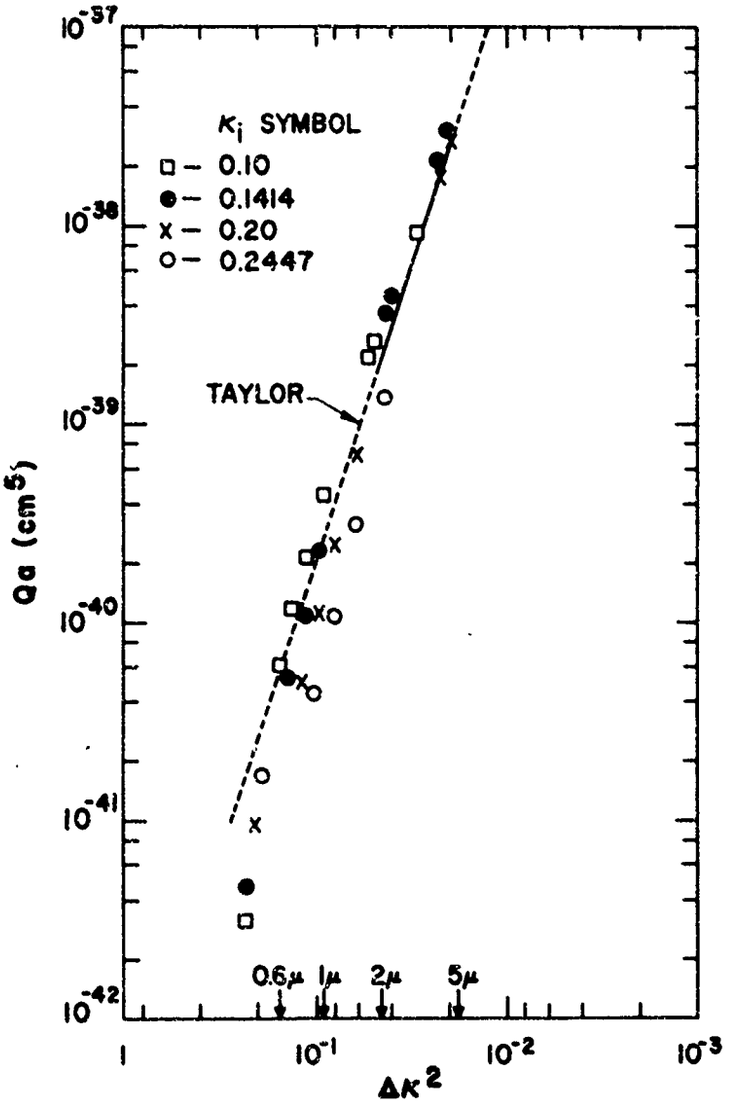

Fig. 5 Bremsstrahlung absorption cross section vs the photon energy in units of $e^2/2a$ for atomic oxygen with $p = 5.2$ and $d^2 = 4.0$. Different exchange force parameters are used for s and p-waves ($\gamma_0 = 1.3$ and $\gamma_1 = 3.4$). Values are shown for four initial wave numbers. The dashed line is an extrapolation of Taylor's measurements using $Z^2 = 0.2 \times 10^{-2}$ with $T = 9000^\circ K$ in the Kramers' formula.

TABLE X

Oxygen Absorption Cross Section for $p = 5.2$, $d^2 = 4.0$, $\gamma_0 = 1.3$ and $\gamma_1 = 3.4$.

κ_i	κ_f	$Q_a(cm^5) \times 10^{40}$	κ_i	κ_f	$Q_a(cm^5) \times 10^{40}$
0.1000	0.1414	1.37E 03	0.2000	0.4000	4.88E-01
0.1000	0.2000	9.34E 01	0.2000	0.5000	9.47E-02
0.1000	0.2449	2.62E 01	0.2449	0.2500	9.88E 04
0.1000	0.2500	2.30E 01	0.2449	0.3194	1.39E 01
0.1000	0.3194	1.36E 00	0.2449	0.3493	3.18E 00
0.1000	0.3493	2.15E 00	0.2449	0.3742	1.09E 00
0.1000	0.3742	1.17E 00	0.2449	0.4000	4.21E-01
0.1000	0.4000	0.07E-01	0.2449	0.5000	1.70E-01
0.1000	0.5000	3.12E-02	0.2500	0.3194	1.57E 01
0.1414	0.2000	2.92E 02	0.2500	0.3493	3.30E 00
0.1414	0.2449	4.41E 01	0.2500	0.3742	1.09E 00
0.1414	0.2500	3.71E 01	0.2500	0.4000	4.12E-01
0.1414	0.3194	4.91E 00	0.2500	0.5000	1.82E-01
0.1414	0.3493	2.21E 00	0.3194	0.3493	1.26E 01
0.1414	0.3742	1.14E 00	0.3194	0.3742	9.11E-01
0.1414	0.4000	5.63E-01	0.3194	0.4000	4.88E-01
0.1414	0.5000	4.70E-02	0.3194	0.5000	5.26E-01
0.2000	0.2449	2.68E 02	0.3493	0.3742	2.89E 00
0.2000	0.2500	1.87E 02	0.3493	0.4000	2.31E 00
0.2000	0.3194	7.17E 00	0.3493	0.5000	9.38E-01
0.2000	0.3493	2.51E 00	0.3742	0.4000	2.93E 01
0.2000	0.3742	1.10E 00	0.3742	0.5000	1.67E 00
			0.4000	0.5000	3.48E 00

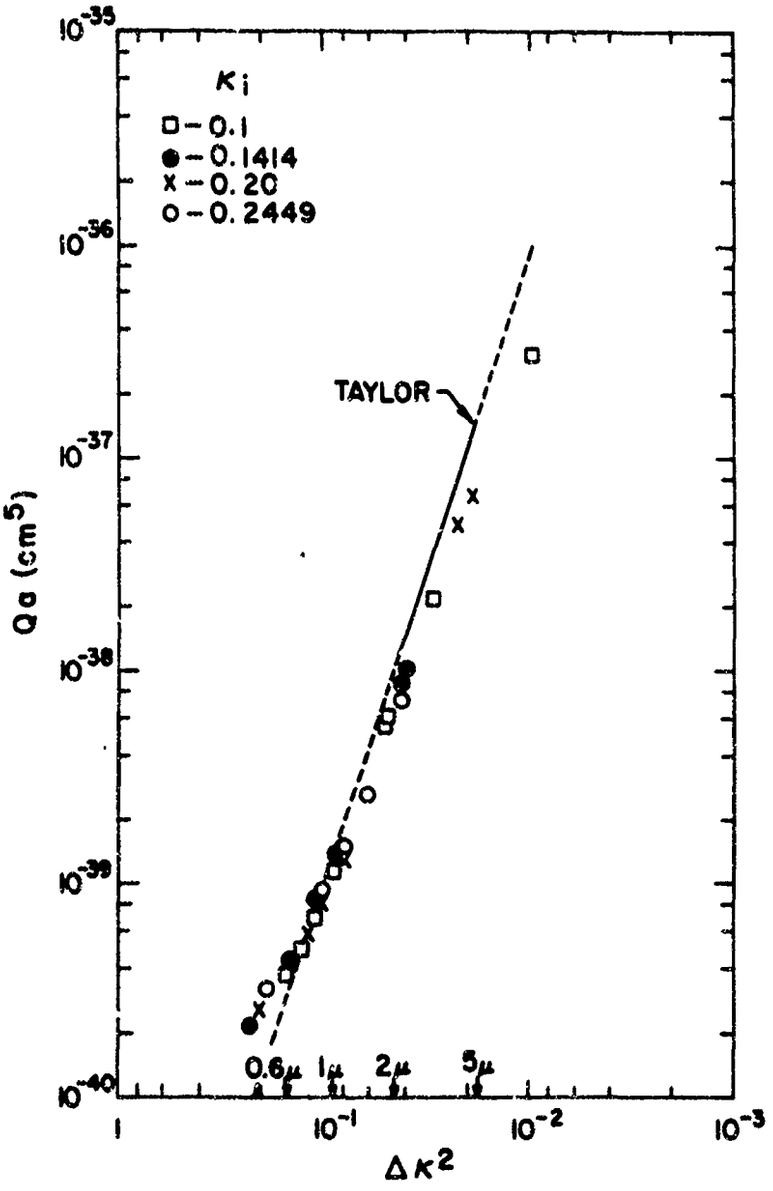

Fig. 6 Bremsstrahlung absorption cross section vs the photon energy in units of $e^2/2a$ for atomic nitrogen with $p = 7.6$ and $d^2 = 5.0$. Different exchange force parameters are used for s and p-waves and for triplet and quintet configurations. Values are shown for four initial wave numbers. The dashed line is an extrapolation of Taylor's meausrements, using $Z^2 = 0.9 \times 10^{-2}$ and T = 9000°K in the Kramers' formula.

TABLE XI

Nitrogen Absorption Cross Section for p = 7.6, d^2 = 5.0.

κ_i	κ_f	$\lambda(\mu)$	$Q_a(cm^5) \times 10^{40}$		
			average	triplet (γ_0 = 0.74, γ_1 = − 0.29)	quintet (γ_0 = 1.79, γ_1 = 4.39)
0.1000	0.1414	9.12	3.09E 03	6.89E 02	4.52E 03
0.1000	0.2000	3.04	2.17E 02	7.31E 01	3.04E 02
0.1000	0.2449	1.82	6.09E 01	3.26E 01	7.79E 01
0.1000	0.2500	1.74	5.35E 01	3.04E 01	6.74E 01
0.1000	0.3194	0.99	1.15E 01	1.50E 01	9.47E 00
0.1000	0.3493	0.81	6.94E 00	1.20E 01	3.88E 00
0.1000	0.3742	0.70	4.94E 00	1.03E 01	1.75E 00
0.1000	0.4000	0.61	3.76E 00	8.85E 00	6.98E-01
0.1000	0.5000	0.38	1.97E 00	5.16E 00	5.34E-02
0.1414	0.2000	4.56	6.77E 02	2.74E 02	9.19E 02
0.1414	0.2449	2.28	1.94E 02	6.55E 01	1.27E 02
0.1414	0.2500	2.15	8.77E 01	5.86E 01	1.05E 02
0.1414	0.3194	1.11	1.41E 01	2.04E 01	1.03E 01
0.1414	0.3493	0.89	8.08E 00	1.52E 01	3.82E 00
0.1414	0.3742	0.76	5.63E 00	1.24E 01	1.60E 00
0.1414	0.4000	0.65	4.22E 00	1.02E 01	5.98E-01
0.1414	0.5000	0.40	2.12E 00	5.46E 00	1.15E-01
0.2000	0.2449	4.56	6.85E 02	5.91E 02	7.42E 02
0.2000	0.2500	4.05	4.83E 02	4.38E 02	5.11E 02
0.2000	0.3194	1.47	2.62E 01	4.58E 01	1.44E 01
0.2000	0.3493	1.11	1.28E 01	2.75E 01	4.02E 00
0.2000	0.3742	0.91	8.24E 00	1.97E 01	1.37E 00
0.2000	0.4000	0.76	5.82E 00	1.48E 01	4.42E-01
0.2000	0.5000	0.43	2.55E 00	6.33E 00	2.84E-01
0.2449	0.2500	36.12	2.94E 05	3.64E 05	2.53E 05
0.2449	0.3194	2.17	7.27E 01	1.50E 02	2.64E 01
0.2449	0.3493	1.47	2.62E 01	6.22E 01	4.61E 00
0.2449	0.3742	1.14	1.45E 01	3.67E 01	1.14E 00
0.2449	0.4000	0.91	9.16E 00	2.39E 01	3.41E-01
0.2449	0.5000	0.48	3.20E 00	7.69E 00	5.09E-01
0.2500	0.3194	2.31	8.64E 01	1.82E 02	2.94E 01
0.2500	0.3493	1.53	2.94E 01	7.04E 01	4.72E 00
0.2500	0.3742	1.18	1.58E 01	4.02E 01	1.11E 00
0.2500	0.4000	0.94	9.81E 00	2.56E 01	3.34E-01
0.2500	0.5000	0.49	3.31E 00	7.91E 00	5.42E-01
0.3194	0.3493	4.56	7.50E 02	1.99E 03	8.32E 00
0.3194	0.3742	2.40	1.29E 02	3.44E 02	8.26E-01
0.3194	0.4000	1.57	4.46E 01	1.17E 02	1.37E 00
0.3194	0.5000	0.62	6.02E 00	1.38E 01	1.37E 00
0.3493	0.3742	5.06	1.28E 03	3.36E 03	2.36E 01
0.3493	0.4000	2.40	1.63E 02	4.20E 02	8.95E 00
0.3493	0.5000	0.71	8.98E 00	2.01E 01	2.27E 00
0.3742	0.4000	4.56	1.17E 03	2.97E 03	1.00E 02
0.3742	0.5000	0.83	1.39E 01	3.06E 01	3.83E 00
0.4000	0.5000	1.01	2.50E 01	5.41E 01	7.55E 00

and, hence, the Maxwell average cross section is independent of temperature and given by the smooth average of the calculated results shown in Fig. 6. The calculated result in the IR is slightly below the result of Taylor shown in Fig. 6 as a solid line determined for a value of $Z^2 = 0.9 \times 10^{-2}$ using Kramers' expression at a temperature of 9000°K. The wavelength dependence of our results deviates from that given by the Kramers' formula (the solid line in Fig. 6). Thus, predictions for atomic nitrogen Bremsstrahlung at 6000 Å if based on Kramers' formulation to extrapolate Taylor's measurements are low by about a factor 2.

7. Summary

Predictions of the Bremsstrahlung absorption cross section for atomic oxygen and nitrogen have been obtained. The results show that there is a consistency between the photo-absorption measurement of the negative oxygen ion and the infrared Bremsstrahlung measurements of Taylor.

In this study the dependence of the exchange force on the configuration of the free electron plus atom has been taken into account. This dependence must be preserved to obtain reasonable results, e.g., in atomic oxygen in which the Bremsstrahlung absorption is small, both s and p-waves are near antiresonance at low electron energy. The same exchange force for s and p-waves does not give this result. It is also necessary in the case of atomic nitrogen to calculate the triplet and quintet absorption coefficients separately since an average force does not give a good representation of the individual p-wave.

The potential that is used in these calculations has only one free parameter, a cut-off for the polarization force (d^2). The value of this parameter has been fixed for oxygen to give agreement with the photo-absorption measurements of the negative oxygen ion. The value of d^2 for atomic nitrogen is obtained by a theoretical scaling technique. The polarizabilities are fixed by experiment and the exchange force parameters are adjusted to be consistent with the Hartree-Fock method.

The magnitude of the Bremsstrahlung predictions are consistent with the infrared measurements of Taylor. The absorption cross section for

atomic oxygen is about a factor 5 less than that of atomic nitrogen. The Maxwell averaged Bremsstrahlung absorption cross section for atomic nitrogen is insensitive to temperature. Its wavelength dependence deviates slightly from that given by the Kramers' expression in that it is relatively larger in the blue. Extrapolations of Taylor's IR measurements using Kramers' formulation may be low by about a factor 2 at 6000 Å.

SECTION II

BREMSSTRAHLUNG IN AIR

1. Introduction

In air, 8000°K and 1 atmosphere of density, the Bremsstrahlung from electrons accelerated in the fields of neutral atoms and molecules contributes about 10 percent of the total (spectrally integrated) emissivity.[1, 2, 3, 4] Recent measurements of infrared radiation from air and nitrogen by Taylor[5] have demonstrated that molecular nitrogen is the most important source of this radiation having about twice the cross section of that of atomic nitrogen.

Unfortunately, the molecular nitrogen, which is the most important source of Bremsstrahlung in high temperature air, is the most difficult to handle theoretically.

In Part 2, the derivation of the quantum mechanical calculation of Bremsstrahlung from a spherically symmetric potential is outlined. In Part 3, a simple approximation relating the Bremsstrahlung to the momentum transfer cross section is given. In Part 4, a calculation by Stier[20] of the elastic scattering of electrons by molecular nitrogen is reviewed. Using a similar approach for Bremsstrahlung, it is shown that the relation between Bremsstrahlung and elastic scattering is as reasonable in the molecular as in the atomic case. In Part 5, a summary of estimates of neutral Bremsstrahlung in high temperature air is given. In addition to the molecular nitrogen the results for molecular oxygen using the same approximation given in Part 3 and justified in Part 4 for molecular nitrogen. The atomic oxygen and nitrogen results are based on recent calculations designed to be consistent with the photo-absorption cross section of negative atomic oxygen.[21]

2. Bremsstrahlung from Low Energy Electrons Scattered by a Spherically Symmetric Potential

Following Nedelsky,[22] the assumption is made that the radiation is proportional to the electron acceleration matrix element squared in an analogy with the classical result

$$J = \frac{4e^2}{3c^3} \left| \underline{a}\, E, E' \right|^2 \qquad (38)$$

Nedelsky, who uses a cut-off Coulomb potential, has the acceleration in the form

$$\underline{a} = - \frac{dV}{dr}\, \underline{j} = - \frac{Ze^2}{mr^2}\, \underline{j} \qquad \text{for } r < a \qquad (39)$$

The initial electron state is determined such that when a unit incident plane wave is subtracted only the outgoing ($e^{\pm ikr}$) waves remain. The final states are composed of both in-going and out-going waves and are normalized so that each component represents one encounter per unit of time.

Although Nedelsky treats this problem in general, the present review is limited to the lowest order waves (s and p waves). Then for the initial state

$$\psi_i \doteq \frac{a_o}{\sqrt{v_i}\ \kappa_i} \left(e^{i\delta_0}\, G_{0i} + 3ie^{i\delta_1} \cos\theta\, G_{1i} \right) \qquad (40)$$

To obtain the total radiation, a summation has to be carried out over the final states and to this low order approximation the final states are

$$\begin{aligned} (\psi_0)_f &= \frac{2}{\sqrt{v_f}} \frac{1}{\sqrt{4\pi}} G_{0f} \\ (\psi_{1,0})_f &= \frac{2}{\sqrt{v_f}} \sqrt{\frac{3}{4\pi}} \cos\theta\, G_{1f} \\ (\psi_{1,\pm 1})_f &= \frac{2}{\sqrt{v_f}} \sqrt{\frac{3}{8\pi}} \sin\theta\, e^{\pm i\phi}\, G_{1f} \end{aligned} \qquad (41)$$

Since the radial vector, $\underset{\sim}{j}$, is

$$\underset{\sim}{j} = \underset{\sim}{i}_x \sin\theta\cos\phi + \underset{\sim}{i}_y \sin\theta\sin\phi + \underset{\sim}{i}_z \cos\theta \tag{42}$$

the radiation is given by

$$J = \frac{64\pi e^6 Z^2}{3c^3 m^2 v_i v_f \kappa_i^2} \left\{ \left| \int_0^a G_{0i}\, G_{1f}\, \frac{1}{r^2}\, dr \right|^2 + \left| \int_0^a G_{1i} G_{0f}\, \frac{1}{r^2}\, dr \right|^2 \right\} \tag{43}$$

The emission cross section is given by

$$Q_e = J/h\nu \tag{44}$$

and using the detailed balance relation between the absorption and emission cross section

$$Q_a = \left(\frac{c^2 v_i^2}{8\pi\nu^2 v_f} \right) Q_e \tag{45}$$

The absorption cross section is found to be

$$Q_a = \frac{256\pi^2}{3} \quad \frac{\alpha a_o^5}{\kappa_i \kappa_f^2 (\Delta\kappa^2)^3} \left\{ \left| \int_0^a G_{0i} G_{1f}\, \frac{Z}{r^2}\, dr \right|^2 + \left| \int_0^a G_{1i} G_{0f}\, \frac{Z}{r^2}\, dr \right|^2 \right\} \tag{46}$$

This is just the expression used by Chandresakar and Breen[28] and others where Z/r^2 is the radial derivative of the potential energy in atomic units.

3. Hundley's Result (Born Approximation)

The close relation between the Bremsstrahlung and the elastic scattering cross sections is seen in the earliest quantum mechanical studies of this problem. Nedelsky,[22] using a cut-off Coulomb potential, found the same maxima and minima as Allis and Morse[23] in the elastic scattering. Thus, the same minima which explained the Ramsauer minimum cross section in argon and krypton indicate in Nedelsky's quantum mechanical calculation that the Bremsstrahlung from low energy electrons will be small for these elements. More recently, Ohmura and Ohmura[24] have related the hydrogen atom Bremsstrahlung to its phase shifts. The validity of this approach for hydrogen has been definitized by the recent calculations of Geltman.[25] Hundley[26] has recently assumed that this may be a generally useful approach and has tried to apply the Born approximation to this problem.

Hundley's relation for the Bremsstrahlung emission is (in the limit $\kappa_i = \kappa_f \equiv \kappa$)

$$\frac{d\sigma}{d\omega} = \frac{16\, e^2 \pi \kappa^2}{3m^2 \omega c^3} \frac{Q_m}{4\pi a_o^2} \tag{47}$$

and Q_m is the momentum transfer cross section. The intensity (J) in the previous section is defined by

$$J = 2\pi h\nu \frac{d\sigma}{d\omega} \tag{48}$$

In applying this result, Hundley suggested using the zero energy scattering length to determine the momentum transfer cross section. Since the low energy nitrogen cross section is apparently fairly small[4] this extension would imply a small molecular nitrogen Bremsstrahlung. However, it seems more reasonable to retain the original momentum transfer cross section in Eq (47) and thereby avoid the question of the low energy limit and extrapolating to the energies of interest.

4. Molecular Nitrogen

A reasonably successful attempt at predicting the elastic scattering of low energy electrons by molecular nitrogen has been given by Stier.[20] Although the model for the electron molecule interaction is crude, it is adjusted on a semi-empirical basis to give the scattering resonance at 2.3 ev so that reasonable agreement is obtained with both the total experimental cross section and its angular distribution. A significant difference between this case and the spherically symmetric one is that the p-wave has two parts depending on the projection of its angular momentum along the internuclear axis of the molecule. This projection is designated by m. There are two important states with ℓ, m values p,σ and p,π. Stier's work indicates that it is the p,σ wave which has a resonance at 2.3 ev.

Stier gives an expression for the elastic scattering cross section in terms of the partial wave phase shifts. It is

$$Q = \frac{4\pi a_o^2}{\kappa^2} \sum_{m \leq \ell} (2-\delta_{0m}) \sin^2 \delta_{\ell,m} \qquad (49)$$

where δ_{0m} is zero except when m equals 0, in which case it is 1. If the phase shift for the two p-waves is the same, then this reduces to the spherically symmetric result $[(2\ell+1) \sin^2 \delta_\ell]$.

In the case of interest for the p-waves, the m = 1 phase shift is negligible, and the remaining contribution to the cross section (m = 0) has a coefficient which is 1/3 of that for the p-wave in spherically symmetric scattering.

Following Stier, a corresponding effect in the Bremsstrahlung relations would be expected. Stier has solved the molecular scattering problem as an expansion in the parameter $\epsilon = d/\lambda$ where d is the nuclear separation in the molecule and λ is $\hbar/mv$, the deBroglie wavelength for the electron.

In the limit of ϵ going to zero, the wave functions are very similar to those encountered in the symmetrical scattering estimate of Bremsstrahlung. The one exception is that the radial part of the p-wave function

now has two parts corresponding to the two values of m. The initial state is,

$$\psi_i \pm \frac{a_o}{\kappa_i \sqrt{v_i}} \left[e^{i\delta_0} (G_0)_i + 3ie^{i\delta_1} (G_{10})_i \right] \qquad (50)$$

where the z-axis is chosen along the direction of the incident plane wave so that only m = 0 occurs. For the final states (as in Part 2) only the four lowest terms are considered

$$(\psi_0)_f = \frac{2}{\sqrt{v_f}} \frac{1}{\sqrt{4\pi}} (G_0)_f$$

$$(\psi_{1,0})_f = \frac{2}{\sqrt{v_f}} \sqrt{\frac{3}{4\pi}} \cos\theta \, (G_{10})_f \qquad (51)$$

$$(\psi_{1,\pm 1})_f = \frac{2}{\sqrt{v_f}} \sqrt{\frac{3}{8\pi}} \sin\theta \, e^{\pm i\phi} (G_{11})_f$$

where $(G_{\ell m})_f$ is the radial function for the ℓ, m wave. Substituting these wave functions into Nedelsky's expression for the intensity gives

$$J = \frac{16\pi}{v_f v_i \kappa_i^2} \left\{ \left| \int_0^\infty (G_{10})_i (G_0)_f \frac{dV}{dr} dr \right|^2 + \frac{1}{3} \left| \int_0^\infty (G_0)_i (G_{10})_f \frac{dV}{dr} \right|^2 \right.$$

$$\left. + \frac{2}{3} \left| \int_0^\infty (G_0)_i (G_{11})_f \frac{dV}{dr} \right|^2 \right\} \qquad (52)$$

As in the elastic scattering, if only the $m = 0$ phase of the $\ell = 1$ states is important, the Bremsstrahlung is reduced by a factor 1/3.

When the incident plane wave is at an angle α with the z-axis, the same result is obtained so that in this approximation the average over angles of incidence gives the same result as taking the incident wave along the z-axis.

It is concluded to this order of approximation that the Bremsstrahlung is proportional to the momentum transfer cross section, even in the non-spherically symmetric case.

5. Results and Summary

As a result of (1) the above study of Bremsstrahlung for molecular nitrogen, (2) the Born approximation as given by Hundley, and (3) our numerical calculations of the atomic oxygen and atomic nitrogen neutral Bremsstrahlung and elastic scattering cross sections,[21] it is concluded that Hundley's approximation should give a reasonable estimate of the Bremsstrahlung absorption cross section.

Using this approximation, the estimates of the neutral Bremsstrahlung from high temperature air can be obtained. The emissivity per unit length is determined according to

$$\frac{\epsilon}{L} = 2N_i N_e Q_a \tag{52}$$

where the density of particles N_i and N_e are taken from the Bureau of Standards results by Hilsenrath et al.[28] The radiation absorption cross section Q_a is determined from the Maxwell averaged momentum transfer cross section Q_m by

$$Q_a = 2.9 \times 10^{-19} Q_m \left(\frac{1.36^{-2}\lambda}{1.24\mu}\right)^3 \frac{4}{\sqrt{\pi}} \left(\frac{T}{11,600 \times 0.544}\right)^{3/2} \tag{53}$$

For the Maxwell average the following has been used:

$$Q_m = \frac{2}{\sqrt{\pi}} \int_0^\infty Q\left(E + \frac{1.24\mu}{2\lambda}\right) \sqrt{u}\, e^{-u}\, du \tag{54}$$

where $u = E/kT$ and E is the initial electron energy. By using measured values of Q and by taking values at $E + (1.24/2\lambda)$, an attempt has been made to take account of the fact that the final state of the electron is at higher energy than the initial state.

With the emissivity per unit length the spectral intensity is calculated according to

$$I_\lambda = \frac{\epsilon}{L} \frac{\sigma T^4}{2\pi 6} \frac{u^4 e^{-u}}{\lambda} \tag{55}$$

where $u = h\nu/kT$.

The results given by Phelps et al.[27] are used for the momentum transfer cross section of molecular nitrogen and of Ramsauer et al.[29] for molecular oxygen. Our calculation of the Bremsstrahlung goes directly to that for atomic oxygen and nitrogen. The results are given in four tables. These contain the intensity (I) in watts/cm^3/ster micron and the emissivity/cm (ϵ/L), i.e., the fraction of the blackbody intensity from 1 centimeter of optical depth. These results are given for temperatures between 5000 and 15,000°K, densities between 10^{-3} and 10 atm and wavelengths between 0.3 and 4.8μ. A sample of these data are plotted in Fig. 7, which gives the intensity for the four neutral species considered as a function of wavelength at T = 9000°K and $\rho/\rho_o = 10$. Also shown is the blackbody limit.

These results are consistent with the measurements of Taylor[5] and the tables of emissivity prepared by Allen[30] based on Taylor's measurements.

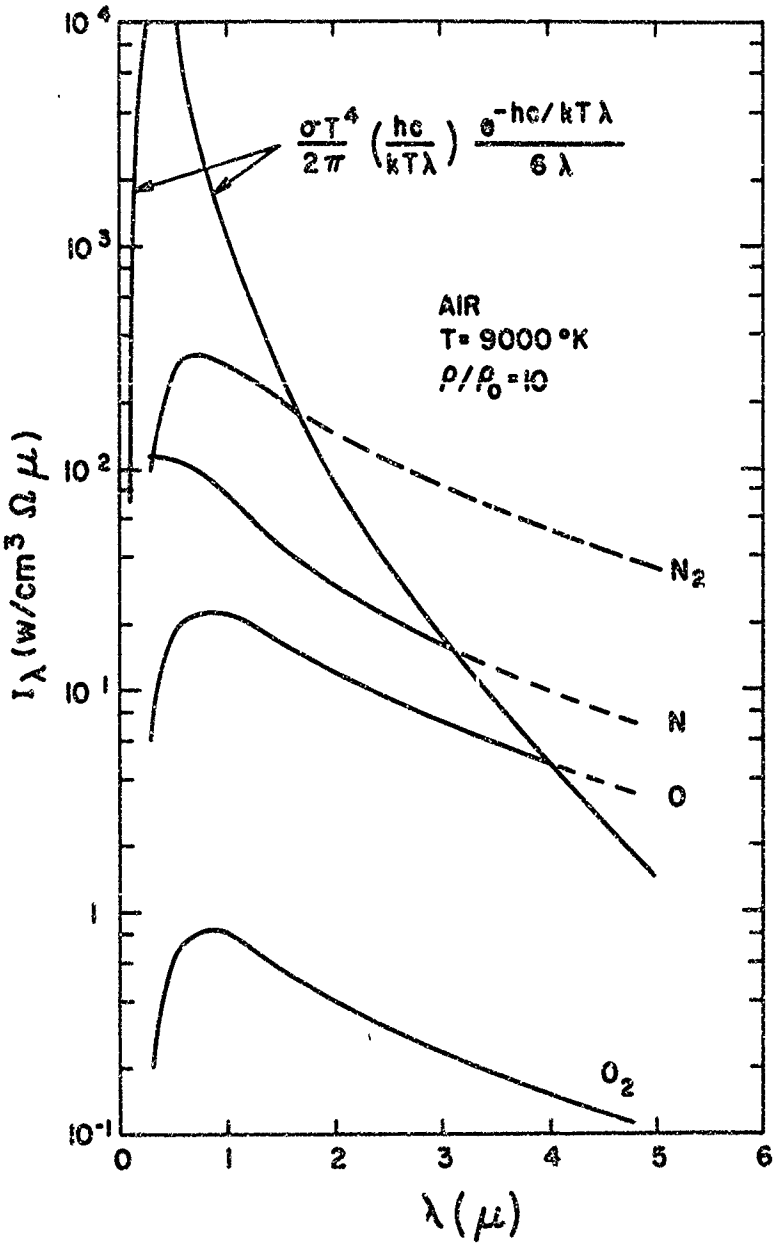

Fig. 7 The spectral intensity in watts per cubic centimeter-steradian-micron as a function of wavelength in microns. The Bremsstrahlung continuum components for molecular N_2 and O_2 and atomic N and O are given separately. Also shown is the corresponding Planck limit. These curves are for a temperature of 9000°K and a density $\rho/\rho_0 = 10$. The component curves are shown as dashed lines when the intensity from 1 cm of optical depth exceeds the Planck limit.

TABLE XII

Bremsstrahlung absorption cross section (Q_a), emissivity per centimeter (ϵ/L) and spectral intensity (I_λ) in watts/cm^3 steradian micron for molecular nitrogen.

T(°K)	λ(μ)	Q_a(cm^5) x 10^{40}	ρ/ρ$_o$ = 0.001		0.01		0.1		1.0		10.0	
			ϵ/L	I_λ	ϵ/L	I_λ	ϵ/L	I_λ	ϵ/L	I_λ	ϵ/L	I_λ
3000	0.3	1.91E-01	4.44E-15	1.32E-15	1.66E-13	4.93E-14	5.52E-12	1.64E-12	1.73E-10	5.13E-11	5.16E-09	1.53E-09
	0.6	7.79E-01	1.80E-14	4.99E-13	6.76E-13	1.87E-11	2.24E-11	6.20E-10	7.03E-10	1.94E-08	2.10E-08	5.80E-07
	1.2	5.00E 00	1.16E-13	5.46E-12	4.34E-12	2.04E-10	1.44E-10	6.79E-09	4.51E-09	2.13E-07	1.35E-07	6.35E-06
	2.4	3.88E 01	8.99E-13	9.78E-12	3.37E-11	3.66E-10	1.12E-09	1.22E-08	3.50E-08	3.81E-07	1.04E-06	1.14E-05
	4.8	2.99E 02	6.93E-12	6.41E-12	2.59E-10	2.40E-10	8.61E-09	7.96E-09	2.70E-07	2.49E-07	8.05E-06	7.45E-06
6000	0.3	4.80E-01	1.61E-11	1.42E-08	1.59E-09	1.41E-06	1.08E-07	9.56E-05	5.91E-06	5.23E-03	2.46E-04	2.18E-01
	0.6	2.74E 00	9.19E-11	1.39E-07	9.08E-09	1.37E-05	6.16E-07	9.30E-04	3.37E-05	5.09E-02	1.40E-03	2.12E 00
	1.2	1.73E 01	5.82E-10	2.03E-07	5.75E-08	2.00E-05	3.90E-06	1.36E-03	2.14E-04	7.44E-02	8.89E-03	3.10E 00
	2.4	1.28E 02	4.30E-09	1.27E-07	4.25E-07	1.26E-05	2.88E-05	8.53E-04	1.58E-03	4.67E-02	6.57E-02	1.94E 00
	4.8	9.83E 02	3.30E-08	5.02E-08	3.26E-06	4.97E-06	2.21E-04	3.37E-04	1.21E-02	1.84E-02	5.04E-01	7.68E-01
9000	0.3	7.74E-01	1.16E-11	1.47E-07	3.76E-09	4.79E-05	9.18E-07	1.17E-02	1.11E-04	1.42E 00	8.01E-03	1.02E 02
	0.6	5.39E 00	8.04E-11	4.60E-07	2.62E-08	1.50E-04	6.39E-06	3.65E-02	7.75E-04	4.43E 00	5.57E-02	3.19E 02
	1.2	3.62E 01	5.41E-10	3.67E-07	1.76E-07	1.19E-04	4.30E-05	2.91E-02	5.21E-03	3.54E 00	3.75E-01	2.54E 02
	2.4	2.69E 02	4.01E-09	1.66E-07	1.31E-06	5.39E-05	3.19E-04	1.32E-02	3.87E-02	1.60E 00	2.78E 00	1.15E 02
	4.8	2.07E 03	3.09E-08	5.56E-08	1.01E-05	1.81E-05	2.45E-03	4.42E-03	2.98E-01	5.36E-01	2.14E 01	3.85E 01
12000	0.3	1.07E 00	2.81E-12	1.36E-07	1.87E-09	9.03E-05	7.59E-07	3.66E-02	2.37E-04	1.14E 01	4.05E-02	1.95E 03
	0.6	8.28E 00	2.17E-11	2.42E-07	1.45E-08	1.61E-04	5.87E-06	6.54E-02	1.83E-03	2.04E 01	3.13E-01	3.49E 03
	1.2	5.87E 01	1.54E-10	1.46E-07	1.02E-07	9.70E-05	4.16E-05	3.94E-02	1.30E-02	1.23E 01	2.22E 00	2.10E 03
	2.4	4.42E 02	1.16E-09	5.66E-08	7.73E-07	3.77E-05	3.14E-04	1.53E-02	9.79E-02	4.77E 00	1.67E 01	8.16E 02
	4.8	3.43E 03	9.00E-09	1.76E-08	5.99E-06	1.17E-05	2.43E-03	4.76E-03	7.59E-01	1.49E 00	1.30E 02	2.54E 02
15000	0.3	1.37E 00	8.83E-14	9.49E-09	4.48E-10	4.82E-05	4.25E-07	4.57E-02	2.04E-04	2.19E 01	7.08E-02	7.60E 03
	0.6	1.13E 01	7.24E-13	1.20E-08	3.68E-09	6.11E-05	3.48E-06	5.79E-02	1.67E-03	2.78E 01	5.80E-01	9.65E 03
	1.2	8.28E 01	5.32E-12	6.16E-09	2.70E-08	3.13E-05	2.56E-05	2.96E-02	1.23E-02	1.42E 01	4.26E 00	4.93E 03
	2.4	6.33E 02	4.07E-11	2.20E-09	2.07E-07	1.11E-05	1.96E-04	1.06E-02	9.39E-02	5.07E 00	3.26E 01	1.76E 03
	4.8	4.94E 03	3.18E-10	6.54E-10	1.61E-06	3.32E-06	1.53E-03	3.15E-03	7.33E-01	1.51E 00	2.56E 02	5.24E 02

TABLE XIII

Bremsstrahlung absorption cross section (Q_a), emissivity per centimeter (ϵ/L) and spectral intensity (I_λ) in watts/cm^3 steradian micron for molecular oxygen.

T(°K)	λ(μ)	Q_a(cm^5) x 10^{40}	ρ/ρ_o = 0.001		0.01		0.1		1.0		10.0	
			ϵ/L	I_λ	ϵ/L	I_λ	ϵ/L	I_λ	ϵ/L	I_λ	ϵ/L	I_λ
3000	0.3	5.29E-02	9.95E-17	2.95E-17	7.78E-15	2.31E-15	3.32E-13	9.86E-14	1.14E-11	3.39E-12	3.45E-10	1.02E-10
	0.6	4.13E-01	7.81E-16	2.16E-14	6.11E-14	1.69E-12	2.61E-12	7.20E-11	8.85E-11	2.45E-09	2.71E-09	7.49E-08
	1.2	3.17E 00	5.97E-15	2.82E-13	4.67E-13	2.20E-11	1.99E-11	9.40E-10	6.77E-10	3.19E-08	2.07E-08	9.77E-07
	2.4	2.37E 01	4.46E-14	4.85E-13	3.49E-12	3.80E-11	1.49E-10	1.62E-09	5.05E-09	5.50E-08	1.55E-07	1.68E-06
	4.8	1.77E 02	3.33E-13	3.08E-13	2.60E-11	2.41E-11	1.11E-09	1.03E-09	3.77E-08	3.49E-08	1.15E-06	1.07E-06
6000	0.3	1.47E-01	1.55E-16	1.37E-13	8.32E-14	7.36E-11	4.37E-11	3.86E-08	1.79E-08	1.58E-05	3.55E-06	3.14E-03
	0.6	1.16E 00	1.22E-15	1.84E-12	6.58E-13	9.92E-10	3.45E-10	5.21E-07	1.42E-07	2.14E-04	2.80E-05	4.23E-02
	1.2	9.03E 00	9.48E-15	3.30E-12	5.10E-12	1.78E-09	2.68E-09	9.33E-07	1.10E-06	3.83E-04	2.18E-04	7.58E-02
	2.4	6.93E 01	7.28E-14	2.15E-12	3.92E-11	1.16E-09	2.06E-08	6.08E-07	8.43E-06	2.50E-04	1.67E-03	4.94E-02
	4.8	5.33E 02	5.59E-13	8.53E-13	3.01E-10	4.59E-10	1.58E-07	2.41E-07	6.48E-05	9.88E-05	1.28E-02	1.95E-02
9000	0.3	2.70E-01	1.22E-15	1.56E-11	4.00E-13	5.09E-09	1.29E-10	1.64E-06	4.45E-08	5.66E-04	1.65E-05	2.10E-01
	0.6	2.14E 00	9.68E-15	5.54E-11	3.17E-12	1.81E-08	1.02E-09	5.85E-06	3.53E-07	2.02E-03	1.30E-04	7.47E-01
	1.2	1.67E 01	7.58E-14	5.14E-11	2.48E-11	1.68E-08	8.00E-09	5.42E-06	2.76E-06	1.87E-03	1.02E-03	6.93E-01
	2.4	1.30E 02	5.89E-13	2.43E-11	1.93E-10	7.96E-09	6.22E-08	2.57E-06	2.15E-05	8.86E-04	7.94E-03	3.28E-01
	4.8	1.01E 03	4.59E-12	8.26E-12	1.50E-09	2.70E-09	4.84E-07	8.72E-07	1.67E-04	3.01E-04	5.18E-02	1.11E-01
12000	0.3	4.18E-01	2.74E-15	1.32E-10	1.50E-12	7.22E-08	5.71E-10	2.76E-05	1.95E-07	9.41E-03	6.12E-05	2.95E 00
	0.6	3.31E 00	2.17E-14	2.42E-10	1.18E-11	1.32E-07	4.51E-09	5.03E-05	1.54E-06	1.72E-02	4.83E-04	5.39E 00
	1.2	2.60E 01	1.70E-13	1.61E-10	9.28E-11	8.79E-08	3.54E-08	3.36E-05	1.21E-05	1.15E-02	3.80E-03	3.60E 00
	2.4	2.09E 02	1.33E-12	6.51E-11	7.27E-10	3.55E-08	2.78E-07	1.35E-05	9.48E-05	4.63E-03	2.98E-02	1.45E 00
	4.8	1.60E 03	1.05E-11	2.05E-11	5.70E-09	1.12E-08	2.18E-06	4.26E-06	7.44E-04	1.46E-03	2.33E-01	4.57E-01
15000	0.3	5.92E-01	5.33E-16	5.73E-11	1.79E-12	1.93E-07	1.29E-09	1.39E-04	5.62E-07	6.04E-02	2.12E-04	2.28E 01
	0.6	4.66E 00	4.19E-15	6.97E-11	1.41E-11	2.35E-07	1.02E-08	1.69E-04	4.42E-06	7.35E-02	1.67E-03	2.78E 01
	1.2	3.67E 01	3.30E-14	3.82E-11	1.11E-10	1.28E-07	8.01E-08	9.27E-05	3.48E-05	4.02E-02	1.31E-02	1.52E 01
	2.4	2.88E 02	2.59E-13	1.40E-11	8.73E-10	4.71E-08	6.30E-07	3.40E-05	2.73E-04	1.47E-02	1.03E-01	5.57E 00
	4.8	2.27E 03	2.04E-12	4.21E-12	6.88E-09	1.42E-08	4.96E-06	1.02E-05	2.15E-03	4.43E-03	8.14E-01	1.67E 00

TABLE XIV

Bremsstrahlung absorption cross section (Q_a), emissivity per centimeter (ϵ/L) and spectral intensity (I_λ) in watts/cm^3 steradian micron for atomic nitrogen.

T(°K)	λ (μ)	Q_a (cm^5) x 10^{40}	ρ/ρ_0 = 0.001		0.01		0.1		1.0		10.0	
			ϵ/L	I_λ	ϵ/L	I_λ	ϵ/L	I_λ	ϵ/L	I_λ	ϵ/L	I_λ
3000	0.3	1.75E 00	6.11E-18	1.81E-18	7.27E-17	2.16E-17	7.64E-16	2.27E-16	7.57E-15	2.25E-15	7.09E-14	2.10E-14
	0.6	3.70E 00	1.29E-17	3.57E-16	1.54E-16	4.25E-15	1.62E-15	4.46E-14	1.60E-14	4.42E-13	1.50E-13	4.14E-12
	1.2	1.80E 01	6.29E-17	2.96E-15	7.48E-16	3.52E-14	7.86E-15	3.70E-13	7.79E-14	3.67E-12	7.30E-13	3.44E-11
	2.4	1.10E 02	3.84E-16	4.18E-15	4.57E-15	4.97E-14	4.80E-14	5.23E-13	4.76E-13	5.18E-12	4.46E-12	4.85E-11
	4.8	8.00E 02	2.80E-15	2.58E-15	3.32E-14	3.07E-14	3.49E-13	3.23E-13	3.46E-12	3.20E-12	3.24E-11	3.00E-11
6000	0.3	1.75E 00	1.64E-10	1.45E-07	3.82E-09	3.38E-06	7.47E-08	6.61E-05	1.27E-06	1.12E-03	1.67E-05	1.48E-02
	0.6	3.70E 00	3.46E-10	5.23E-07	8.08E-09	1.22E-05	1.58E-07	2.38E-04	2.68E-06	4.04E-03	3.54E-05	5.34E-02
	1.2	1.80E 01	1.69E-09	5.87E-07	3.93E-08	1.37E-05	7.69E-07	2.68E-04	1.30E-05	4.54E-03	1.72E-04	6.00E-02
	2.4	1.10E 02	1.03E-08	3.05E-07	2.40E-07	7.10E-06	4.70E-06	1.39E-04	7.95E-05	2.36E-03	1.05E-03	3.11E-02
	4.8	8.00E 02	7.49E-08	1.14E-07	1.75E-06	2.66E-06	3.42E-05	5.21E-05	5.79E-04	8.83E-04	7.65E-03	1.17E-02
9000	0.3	1.75E 00	2.47E-08	3.15E-04	8.01E-07	1.02E-02	2.25E-05	2.87E-01	4.77E-04	6.07E 00	8.71E-03	1.11E 02
	0.6	3.70E 00	5.23E-08	2.99E-04	1.69E-06	9.70E-03	4.77E-05	2.73E-01	1.01E-03	5.77E 00	1.84E-02	1.05E 02
	1.2	1.80E 01	2.55E-07	1.73E-04	8.24E-06	5.59E-03	2.32E-04	1.57E-01	4.91E-03	3.33E 00	8.96E-02	6.08E 01
	2.4	1.10E 02	1.56E-06	6.42E-05	5.04E-05	2.08E-03	1.42E-03	5.85E-02	3.00E-02	1.24E 00	5.48E-01	2.26E 01
	4.8	8.00E 02	1.13E-05	2.04E-05	3.66E-04	6.60E-04	1.03E-02	1.86E-02	2.18E-01	3.93E-01	3.98E 00	7.17E 00
12000	0.3	1.75E 00	1.68E-07	8.13E-03	8.35E-06	4.03E-01	3.10E-04	1.50E 01	1.00E-02	4.85E 02	2.43E-01	1.17E 04
	0.6	3.70E 00	3.56E-07	3.97E-03	1.77E-05	1.97E-01	6.56E-04	7.31E 00	2.12E-02	2.37E 02	5.14E-01	5.73E 03
	1.2	1.80E 01	1.73E-06	1.64E-03	8.59E-05	8.13E-02	3.19E-03	3.02E 00	1.03E-01	9.78E 01	2.50E 00	2.37E 03
	2.4	1.10E 02	1.06E-05	5.16E-04	5.25E-04	2.56E-02	1.95E-02	9.52E-01	6.31E-01	3.08E 01	1.53E 01	7.48E 02
	4.8	8.00E 02	7.70E-05	1.51E-04	3.82E-03	7.47E-03	1.42E-01	2.78E-01	4.59E 00	8.99E 00	1.11E 02	2.18E 02
15000	0.3	1.74E 00	1.10E-07	1.18E-02	1.85E-05	1.99E 00	1.15E-03	1.23E 02	4.81E-02	5.17E 03	1.73E 00	1.86E 05
	0.6	3.70E 00	2.33E-07	3.88E-03	3.91E-05	6.50E-01	2.42E-03	4.03E 01	1.02E-01	1.69E 03	3.65E 00	6.07E 04
	1.2	1.80E 01	1.13E-06	1.31E-03	1.90E-04	2.20E-01	1.18E-02	1.36E 01	4.95E-01	5.72E 02	1.78E 01	2.05E 04
	2.4	1.10E 02	6.93E-06	3.74E-04	1.16E-03	6.27E-02	7.21E-02	3.89E 00	3.02E 00	1.63E 02	1.03E 02	5.85E 03
	4.8	8.00E 02	5.04E-05	1.04E-04	8.45E-03	1.74E-02	5.24E-01	1.08E 00	2.20E 01	4.52E 01	7.80E 02	1.62E 03

TABLE XV

Bremsstrahlung absorption cross section (Q_λ), emissivity per centimeter (ϵ/L) and spectral intensity (I_λ) in watts/cm^3 steradian micron for atomic oxygen.

$T(^\circ K)$	$\lambda(\mu)$	$Q_\lambda(cm^5) \times 10^{40}$	ρ/ρ_0 = 0.001		0.01		0.1		1.0		10.0	
			ϵ/L	I_λ	ϵ/L	I_λ	ϵ/L	I_λ	ϵ/L	I_λ	ϵ/L	I_λ
3000	0.3	7.80E-01	6.30E-16	1.87E-16	1.09E-14	3.21E-15	1.29E-13	3.83E-14	1.33E-12	3.95E-13	1.26E-11	3.75E-12
	0.6	6.10E-01	4.92E-15	1.36E-13	8.47E-14	2.34E-12	1.01E-12	2.79E-11	1.04E-11	2.88E-10	9.88E-11	2.73E-09
	1.2	5.00E 00	4.04E-14	1.90E-12	6.94E-13	3.27E-11	8.27E-12	3.90E-10	8.53E-11	4.02E-09	8.10E-10	3.82E-08
	2.4	4.00E 01	3.23E-13	3.52E-12	5.55E-12	6.04E-11	6.62E-11	7.20E-10	6.82E-10	7.43E-09	6.48E-09	7.06E-08
	4.8	3.15E 02	2.54E-12	2.35E-12	4.37E-11	4.04E-11	5.21E-10	4.82E-10	5.37E-09	4.97E-09	5.10E-08	4.72E-08
6000	0.3	7.80E-02	3.25E-12	2.97E-09	1.83E-10	1.61E-07	9.93E-09	8.78E-06	4.61E-07	4.08E-04	1.33E-05	1.17E-02
	0.6	6.10E-01	2.62E-11	3.96E-08	1.43E-09	2.15E-06	7.76E-08	1.17E-04	3.60E-06	5.44E-03	1.04E-04	1.57E-01
	1.2	5.00E 00	2.15E-10	7.49E-08	1.17E-08	4.06E-06	6.36E-07	2.22E-04	2.95E-05	1.03E-02	8.52E-04	2.97E-01
	2.4	4.00E 01	1.72E-09	5.09E-08	9.36E-08	2.77E-06	5.09E-06	1.51E-04	2.36E-04	6.99E-03	6.81E-03	2.02E-01
	4.8	3.15E 02	1.35E-08	2.07E-08	7.37E-07	1.12E-06	4.01E-05	6.11E-05	1.86E-03	2.84E-03	5.37E-02	8.18E-02
9000	0.3	7.80E-02	3.00E-10	3.82E-06	9.82E-09	1.25E-04	3.18E-07	4.04E-03	1.13E-05	1.44E-01	4.70E-04	5.98E 00
	0.6	6.10E-01	2.35E-09	1.34E-05	7.68E-08	4.39E-04	2.48E-06	1.42E-02	8.87E-05	5.07E-01	3.67E-03	2.10E 01
	1.2	5.00E 00	1.92E-08	1.30E-05	6.29E-07	4.27E-04	2.04E-05	1.38E-02	7.27E-04	4.93E-01	3.01E-02	2.04E 01
	2.4	4.00E 01	1.54E-07	6.35E-06	5.03E-06	2.08E-04	1.63E-04	6.72E-03	5.81E-03	2.40E-01	2.41E-01	9.95E 00
	4.8	3.15E 02	1.21E-06	2.10E-06	3.97E-05	7.14E-05	1.28E-03	2.31E-03	4.58E-02	8.25E-02	1.90E 00	3.42E 00
12000	0.3	7.80E-02	2.36E-09	1.14E-04	1.06E-07	5.11E-03	3.81E-06	1.84E-01	1.29E-04	6.23E 00	4.64E-03	2.05E 02
	0.6	6.10E-01	1.84E-08	2.06E-04	8.27E-07	9.22E-03	2.98E-05	3.32E-01	1.01E-03	1.12E 01	3.32E-02	3.70E 02
	1.2	5.00E 00	1.51E-07	1.43E-04	6.78E-06	6.42E-03	2.44E-04	2.31E-01	8.27E-03	7.83E 00	2.72E-01	2.57E 02
	2.4	4.00E 01	1.21E-06	5.90E-05	5.42E-05	2.65E-03	1.95E-03	9.53E-02	6.62E-02	3.23E 00	2.18E 00	1.06E 02
	4.8	3.15E 02	9.52E-06	1.86E-05	4.27E-04	8.36E-04	1.54E-02	3.01E-02	5.21E-01	1.02E 00	1.71E 01	3.35E 01
15000	0.3	7.80E-02	2.03E-09	2.18E-04	2.77E-07	2.98E-02	1.50E-05	1.61E 00	5.98E-04	6.42E 01	2.24E-02	2.41E 03
	0.6	6.10E-01	1.59E-08	2.64E-04	2.17E-06	3.60E-02	1.17E-04	1.95E 00	4.68E-03	7.77E 01	1.75E-01	2.91E 03
	1.2	5.00E 00	1.30E-07	1.50E-04	1.78E-05	2.07E-02	9.60E-04	1.11E 00	3.83E-02	4.43E 01	1.44E 00	1.66E 03
	2.4	4.00E 01	1.04E-06	5.61E-05	1.42E-04	7.66E-03	7.68E-03	4.14E-01	3.07E-01	1.65E 01	1.15E 01	6.20E 02
	4.8	3.15E 02	8.19E-06	1.69E-05	1.12E-03	2.30E-03	6.05E-02	1.25E-01	2.41E 00	4.97E 00	9.05E 01	1.86E 02

SECTION III
SYNCHRONIZED HIGH-SPEED SCANNING INFRARED SPECTROMETER

1. Introduction

The spectral radiation intensity of a short duration radiation source is usually measured using a spectrograph or a multichannel spectrometer. When the spectral radiation intensity varies in times of the order of 10 to 50 μ sec, such as in shock tubes, spectrographs must be equipped with drum cameras or high speed shutters in order to provide time resolution. However, the uncertainties inherent in quantitative analysis of spectrograms and the limited sensitivity and spectral range of emulsions usually result in spectrographs being used only for qualitative analysis. More suitable are multichannel spectrometers which provide continuous radiation histories for a number of adjacent wavelength bands. However, with these instruments, a number of stable detector-recorder systems must be simultaneously maintained, and the resulting spectrum contains discontinuities between each adjacent band.

The disadvantages of the above-mentioned systems are avoided by using a scanning spectrometer which is synchronized with the source. Many varieties of rapid scanning spectrometers have been built,[31-44] employing various methods of scanning the spectrum including electronic scanning, movement of one of the optical components, or movement of the slit. These instruments either scan a narrow spectral region with good spectral resolution or a wide spectral region with more modest resolution. Photomultipliers or electronic storage devices are used as detectors in the visible spectral region while the fast response photoconductive detectors have been used in the infrared. A synchronized high speed scanning infrared spectrometer of novel design will be described in this report. The instrument was built to operate in the infrared region from 2 to 6 microns scanning a spectral region 0.6 microns wide in 30μ sec.

In the following Parts of this report the instrument will be described and its performance presented. In order to illustrate the chief advantages

of this spectrometer, its high scanning rate and its time syncronization with short duration sources, a brief description will be given of the use of the instrument to obtain radiation data on gases heated to high temperature in shock tubes.

2. Description Of The Instrument

The spectrometer consists of an f/12 Ebert type monochromator with a scanning mirror placed 2 inches before the exit slit, as shown in Fig. 8. An infrared detector* with a sensitive area 0.3 x 5 mm acts as the exit slit, although a separate slit and a large detector area could also be used. Since this instrument was built to survey the infrared emission from high-temperature, shock-heated gases, it was decided to sacrifice resolution in order to scan an appreciable portion of the infrared spectrum in times commensurate with the experiment. A total scan of 0.6 μ in 30 μsec, or a scanning rate of 0.02 μ/ μsec, was desired. To achieve this within the basic deisgn of the spectrometer, a grating ruled with 10 grooves/mm was necessary to obtain an inverse linear dispersion of 0.2 μ/mm. The blaze wavelength of the grating was chosen to maximize the signal-to-noise ratio in the region 2-6 μ, taking into account the manufacturer's sensitivity curve for the indium antimonide detector.[45] The final grating used in the instrument was a 5.8-cm square magnesium grating with 10 grooves/mm, $\lambda_{Blaze} \sim 3\ \mu$, and $\theta_{Blaze} \sim 1^{\circ}$.**

In order to achieve wavelength scanning the scanning mirror is spun by a magnetic field created when a current pulse is passed through a coil surrounding the mirror. The mirror accelerates for about 15 μsec and then coasts with a constant ratational velocity producing a linear scanning rate of about 0.1 mm per μsec. Since the inverse linear dispersion is 0.2 μ/mm, the spectral scanning rate is 0.02 μ/μsec.

---

*Philco Model ISC 301 D and Texas Instruments Model ISV liquid nitrogen cooled indium antimonide detectors have been used.

**Ruled by Bausch and Lomb.

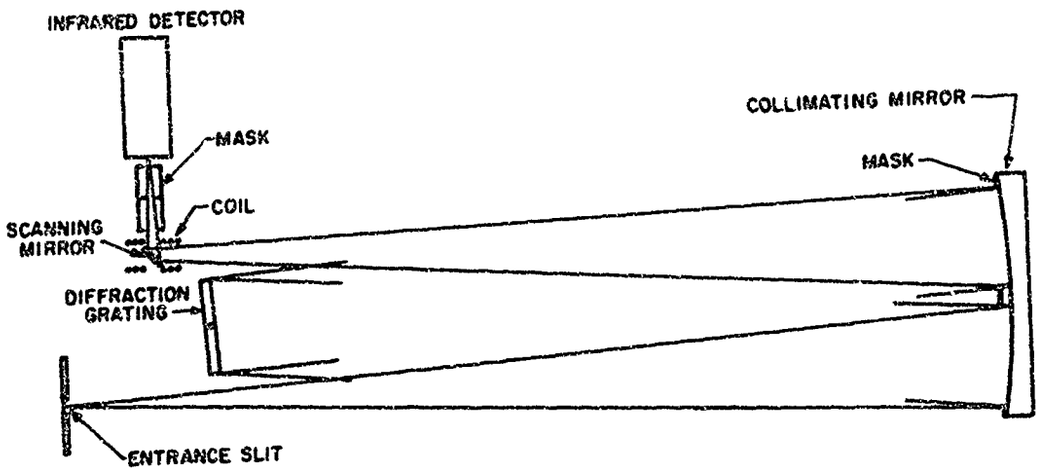

Fig. 8 Schematic diagram (side view) of the synchronized high speed scanning spectrometer. The basic spectrometer is an Ebert type instrument with an aluminum scanning mirror placed 2 inches before the exit slit (IR detector).

The scanning mirror consists of an aluminum disk 0.31 inch in diameter and 0.04 inch-thick, on each face of which aluminum mirrors are replicated as follows. A recess 0.005 inch deep is cut into each face of the disk leaving a 0.010 inch-thick rim. A drop of epoxy cement was used in the recess to cement the disk to a freshly aluminized optical flat. Upon separation of the disk from the optical flat the aluminum surface remained attached to the disk. By this technique, good quality mirror surfaces are easily produced.

The mirror is supported inside a split 6-turn coil by two pivots, one of which is hollow. The coil is potted to provide rigidity, and the pivots are screwed into the coil assembly. The mirror may be rotated manually by means of a knob attached by bevel gears to a wire inserted through the hollow pivot and pressed into a rubber sleeve mounted in the bearing hole in the mirror. The rubber sleeve is attached to and rotates with the mirror. This arrangement provides a small amount of friction to move the mirror manually, but not enough to impede the rotation of the mirror during scanning.

The current pulse that passes through the coil is provided by a single shot, pulse generator, consisting essentially of a 60 μf capacitor which can be charged to 800 volts. The current is dumped across the coil by triggering a thyratron tube with an external electrical pulse, such as the gate pulse from an oscilloscope.

In order to accurately indicate the wavelength while scanning, a wavelength calibration signal generator was incorporated into the instrument. The signal is produced by a photomultiplier in front of which is placed a linear grid. A line light source is imaged by a concave mirror onto this grid after being reflected twice from the back face of the scanning mirror as is schematically shown in Fig. 9. As the scanning mirror rotates, the image of the source travels across the grid causing radiation to fall intermittently on the photomultiplier. The spaces in the grid are equidistant, with the exception that the spaces immediately adjacent to the central or "index" space have been blocked so as to enable accurate identification of the index signal. The normal distance between the spaces in the grid corresponds to a wavelength interval of 0.0224 μ. The output of the

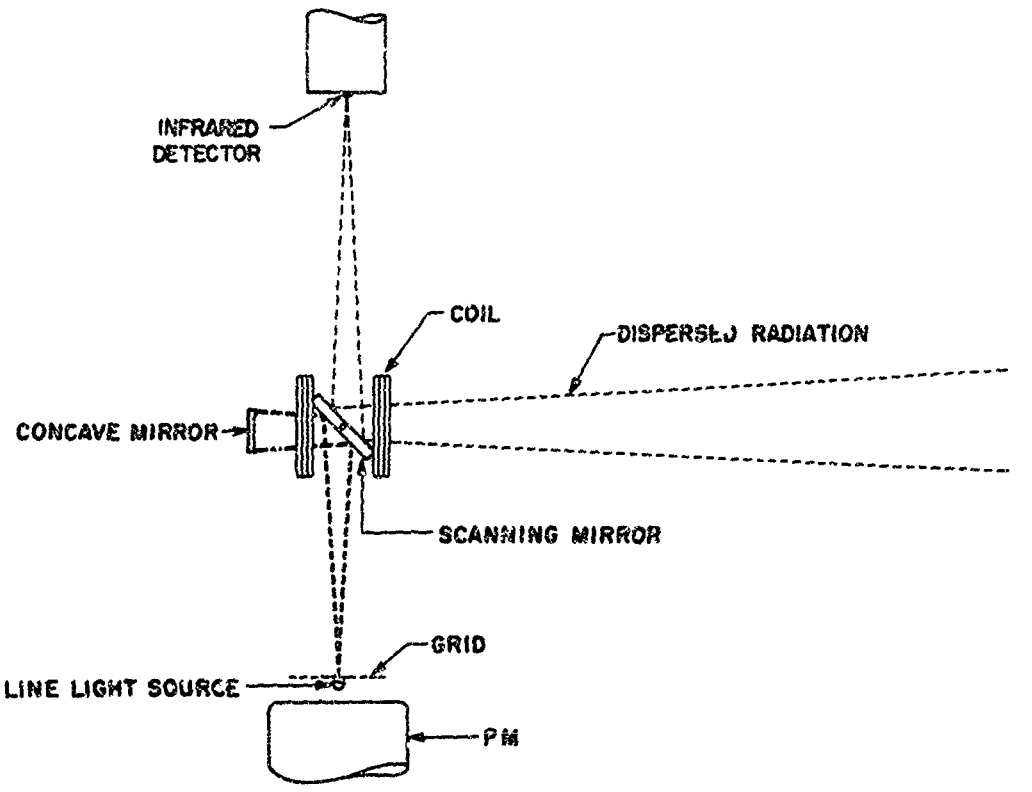

Fig. 9 Schematic diagram of the scanning mirror assembly nd wavelength calibration signal generator. The dispersed radiation enters from the right and is deflected by the upper surface of the scanning mirror to the infrared detector at the top of the figure. The line light source of the wavelength calibration signal generator is at the bottom of the figure. This light is reflected twice off the bottom side of the scanning mirror and is brought to focus on a grid placed in front of a photomultiplier. Rotation of the scanning mirror causes the light to move across the grid generating a series of pulses which can be used to measure the angular position of the mirror and hence the wavelength of the radiation falling on the IR detector.

wavelength calibration signal generator is recorded simultaneously with the infrared detector signal on a dual beam oscilloscope thus providing a calibrated wavelength scale with each scan.

The grating can be rotated to obtain the desired wavelength band, and a dial indicator has been provided to show the grating position. This dial has been calibrated to indicate the wavelength falling on the exit slit for the index position of the scanning mirror. The calibration was accomplished by using the instrument to scan various known bands of molecules in absorption. For example, Fig. 10 (a) shows the oscillogram obtained by scanning the 3.04 μ absorption band of 306 torr of C_2H_2 contained in a 10-cm path length cell using a 1000°K blackbody source. The lower trace on the oscillogram shows the wavelength calibration signal including the prominent index signal. Figure 3 (b) shows a similar absorption trace of the 4.26 μ band of CO_2. This was obtained from the air in the optical path of the instrument. In normal operation, the spectrometer is flushed with dry N_2 to eliminate such absorption from atmospheric components CO_2 and H_2O. By using various gases, films, and narrow band interference filters, a calibration curve covering the useful range of the instrument was constructed and is shown in Fig. 11.

The combination of linear dispersion and detector width provide a theoretical spectral resolution of 0.06 μ. Measurements made by scanning lines and bands indicate that the experimental resolution is 0.07 μ. The response time of the infrared detector was experimentally measured using a radiation chopper built at this laboratory which can produce trapezoidal shaped light pulses of 1-2 μsec duration with total rise times of 0.1-0.2 μsec. From this information the response time (90% of total rise) of the detector-electronic system was adjusted to be about 2.5 μsec, which provides the maximum integration and hence signal for the given spectral resolution and scanning rate.

3. Performance

Prior to operation of the spectrometer the scanning mirror is set visually so that the image of the wavelength calibration source is on the short wavelength side of the grid. The image of the source is easily observed inside the spectrometer through a window in the side of the instrument casing.

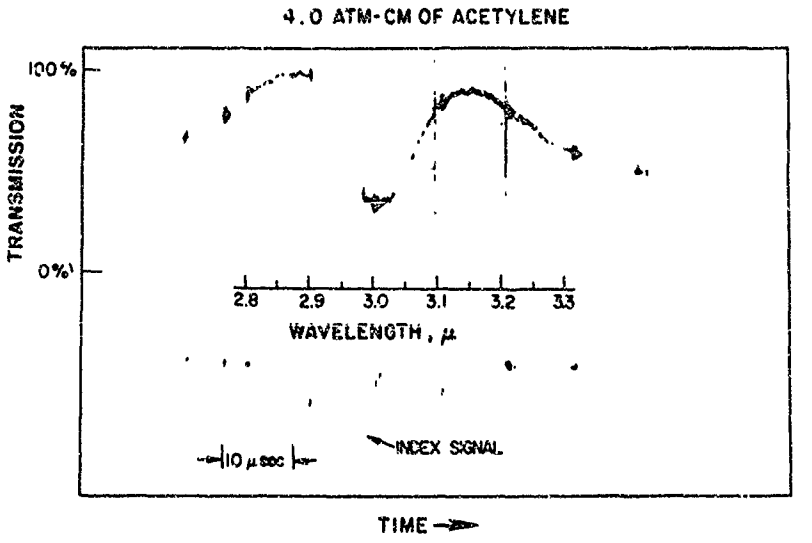

(a) The top trace is from the IR detector and shows the absorption produced by 4.0 atm-cm of acetylene. The bottom trace is the wavelength calibration signal and has been used to produce the wavelength scale shown on the oscillogram.

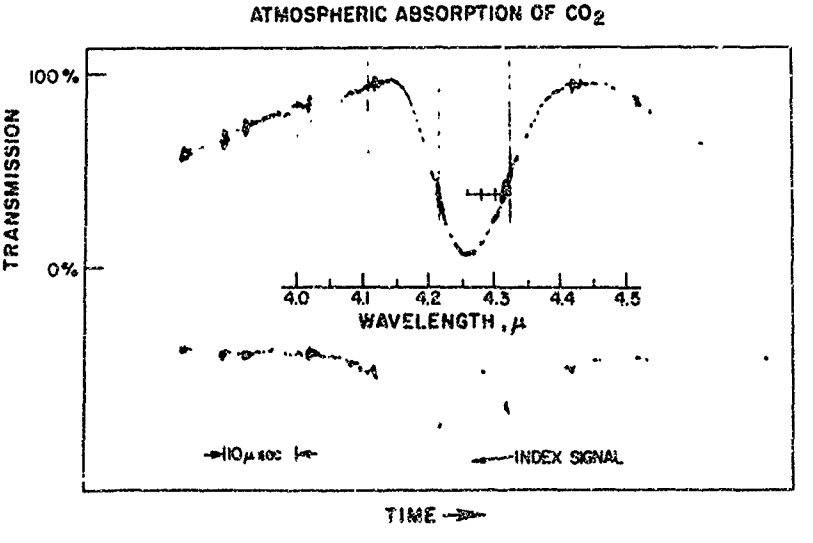

(b) The two traces have the same meaning as in (a) but the absorption is caused by the atmospheric CO_2 in the optical path.

Fig. 10 Typical scans of molecular absorption bands. The radiation source was a 1000°K blackbody.

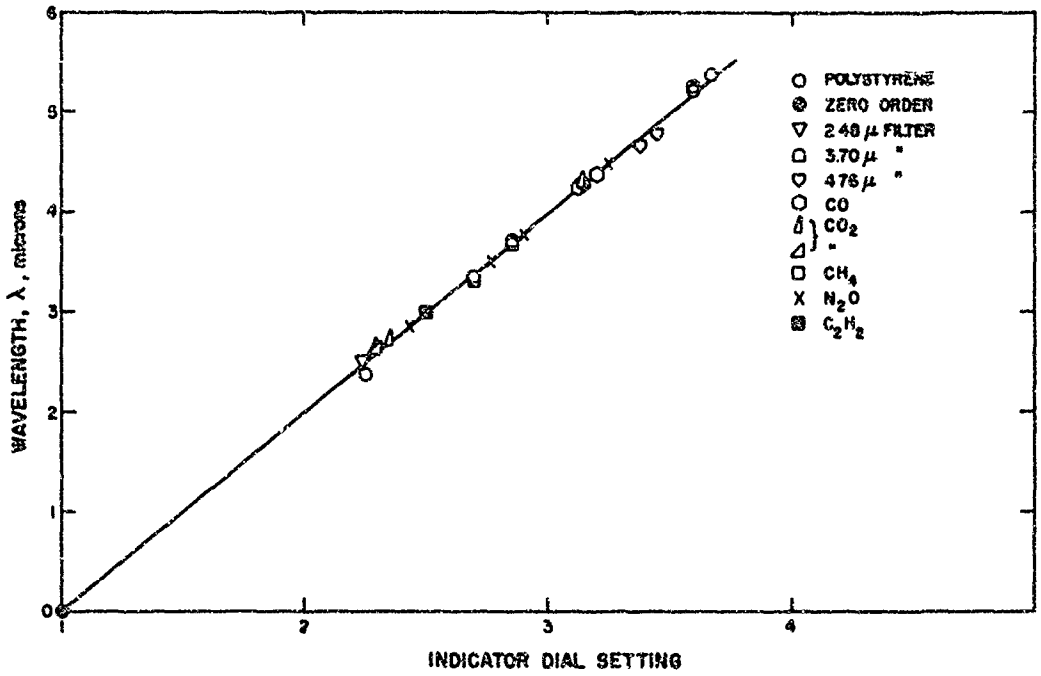

Fig. 11 Wavelength calibration curve for the scanning spectrometer. All the data points are wavelengths determined by scanning molecular absorption bands of gases or polystyrene film or from scanning interference filters. The solid line is a theoretical curve determined from the grating characteristics and the dimensions of the instrument.

On triggering, the capacitor is then discharged through the coil spinning the mirror and causing the spectrum to move across the exit slit. The mirror must then be reset for the next measurement. The output of the detector and wavelength calibration signal generator are recorded simultaneously on a dual beam oscilloscope, as illustrated by the C_2H_2 and CO_2 absorption signals shown in Fig. 10.

Time measurements on the wavelength calibration signal provide data from which the rotational velocity history of the scanning mirror can be determined. The rotational velocity of the mirror in revolutions per second is plotted against time after the initiation of the discharge of the current through the coil as shown in Fig. 12. The mirror is seen to accelerate for about 17 μsec, and to coast at a constant rotational velocity. The spectral data is obtained during the first rotation just after the mirror has reached constant velocity.

In order to make absolute spectral measurements with this instrument, it was necessary to calibrate the spectrometer against a standard source. An absolute spectral sensitivity curve, shown in Fig. 13, was obtained by using a 1000°K blackbody source with the scanning mirror held fixed in its index position. The blackbody was focused on the entrance slit of the spectrometer with the same optical system as used on the shock tube. High-pass filters at 0.9 μ and 2.8 μ were used when needed to eliminate higher orders. The linearity of the detector and electronics were also checked by varying the blackbody source temperature and the entrance slit width.

A difficulty associated with many scanning instruments that use rotating mirrors is that the optical path is vignetted as the mirror turns. This problem is inherent in the current instrument, but has been accounted for by establishing an experimental vignette correction as shown in Fig. 14. The vignette correction was determined in two different ways. Scans of the blackbody source at 1000°K were compared to the "static" calibration curve, Fig. 13. The ratio of the static calibration signal taken with the mirror at its index position to the scan signal at the same wavelength is the vignette correction factor. In order to assure that there are no vignette factors that arise only when the mirror is pulsed, e.g., due to distortion

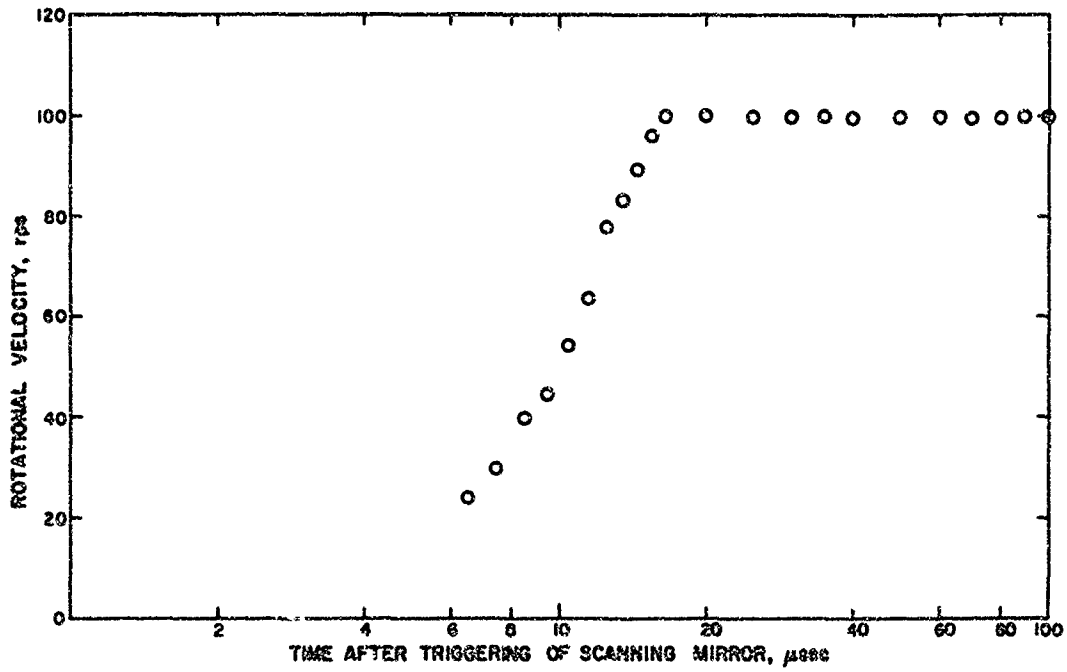

Fig. 12 Plot of the rotational velocity of the scanning mirror versus time after the initiation of the current pulse through the coil that surrounds the mirror. The mirror is seen to accelerate for about 17μsec and then rotates at a constant velocity of about 100 rps. Spectral data are taken during the constant velocity region.

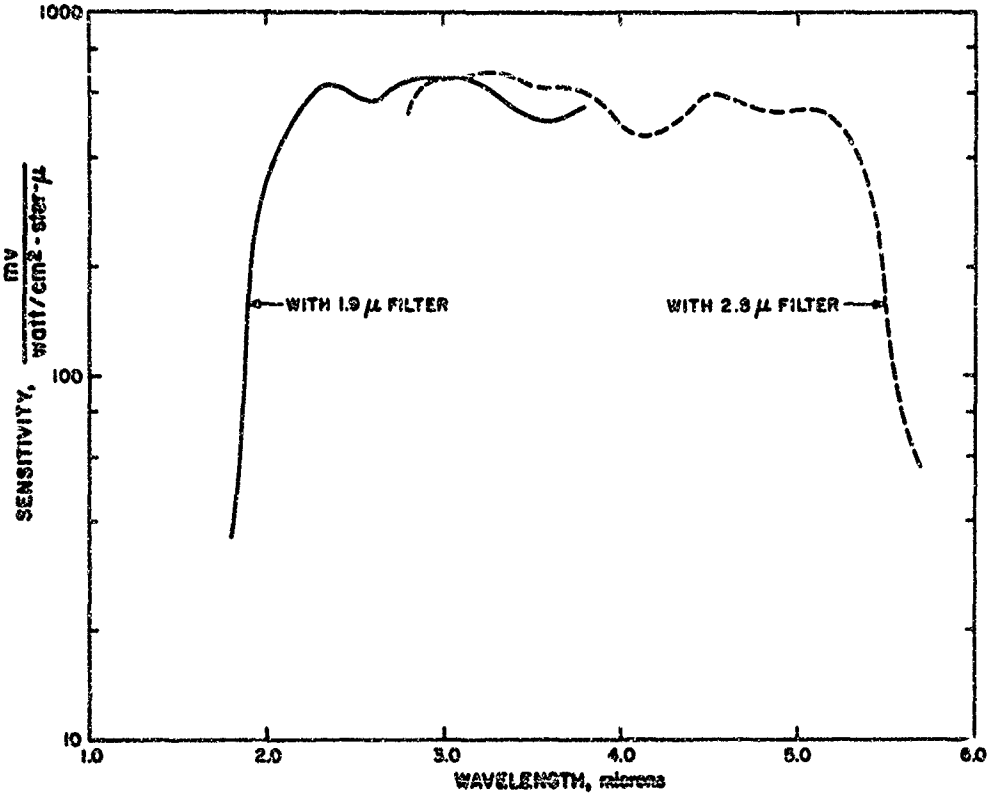

Fig. 13 Absolute spectral sensitivity curve for the infrared scanning spectrometer. The source used was a 1000°K blackbody. The calibration was performed using the shock tube optical system. The different curves are for two spectral regions using two different blocking filters to eliminate higher order radiation.

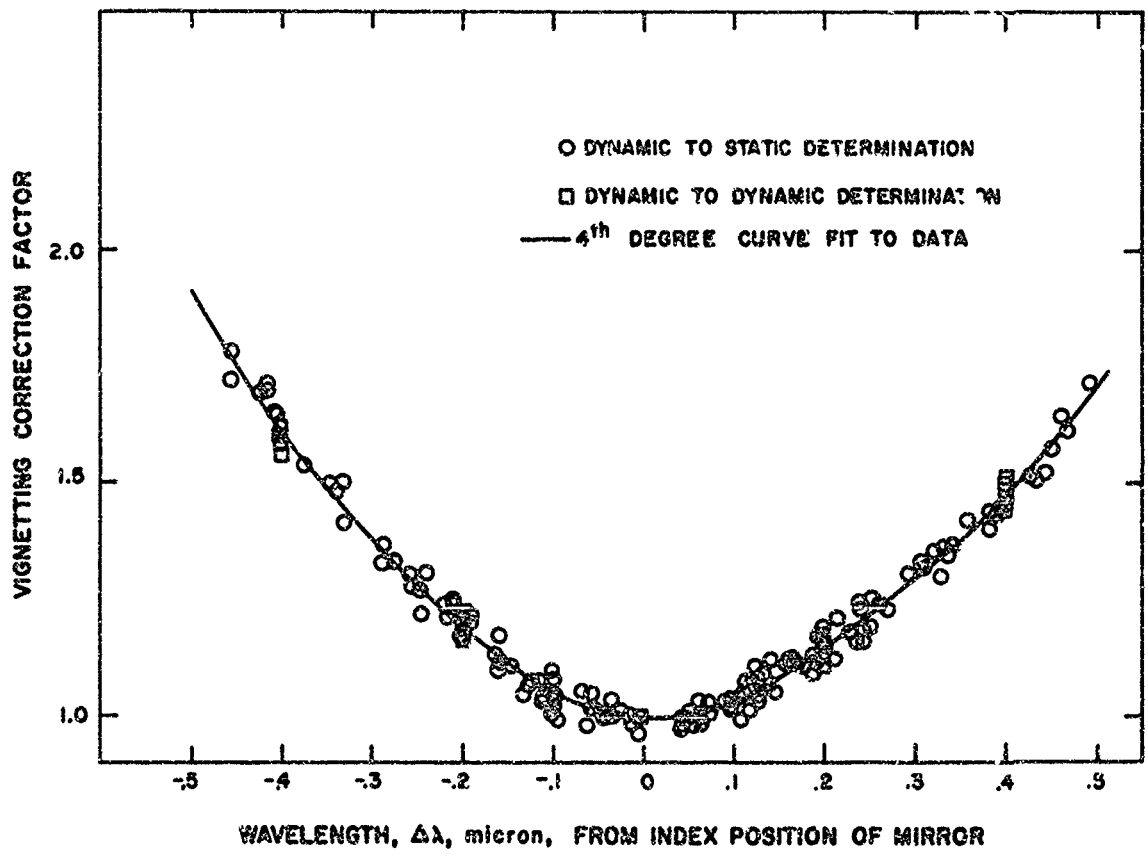

Fig. 14 Experimentally determined vignetting correction factor as a function of $\Delta\lambda$ from the index position of the scanning mirror. The vignetting correction factor was determined by a comparison of dynamic (scanning) data to static data, O; and also by comparing dynamic to dynamic data, □. The solid curve is a 4th degree curve fit to the data and is used for data analyses.

of the scanning mirror, the correction factor was also determined from purely dynamic data. Scans were made of the same source at slightly different wavelength settings. The ratio of the signal at the index position of one scan to the signal at the same wavelength on the other scan, is again the vignetting correction factor. As seen in Fig. 14, the results of both of these methods agree within the scatter of the data. The vignette factor is also observed to be symmetric about the index position of the mirror. The curve in Fig. 14 is a 4th degree curve fit to the data which is the actual vignette correction factor used in data reduction.

In the present experiments using this scanning spectrometer on a shock tube, the test time varied from 30 to 50 μsec. It is obviously desirable to synchronize the spectrometer with the arrival of the shock wave at the test station so as to use that portion of the scan with minimum vignette correction. It has proved easy to accomplish this synchronization in actual practice so that the maximum vignette correction was not more than 1.50 on any shock tube run and generally of the order of 1.25 to 1.30.

4. Use Of The Instrument

The scanning infrared spectrometer described in this paper has been used on a shock tube to measure the spectral radiation intensities of air, nitrogen, argon, and neon heated by reflected shocks. The shock tube was a conventional, combustion-driven tube; the driven section was of square cross section 1.37 inches wide and 10 feet long. The spectrometer was positioned to view the shock-heated gas through a 0.080 inch thick sapphire window in a direction perpendicular to the shock tube axis about 1 inch from the end wall as shown in Fig. 15. A photomultiplier used for monitoring the shocked gas and for timing was positioned on the opposite side of the test section from the spectrometer. It was used with a slit system that restricted its field of view to the same region of test gas as was viewed by the spectrometer. This photomultiplier has an S-1 cathode and was sensitive to a broad band of radiation in the near infrared.

Figure 15 also illustrates the method of displaying data for these shock tube runs. The oscilloscopes (a) and (b) are triggered from a heat transfer gauge located approximately 13 inches upstream from the end wall of the tube after a fixed delay which is varied depending upon the expected

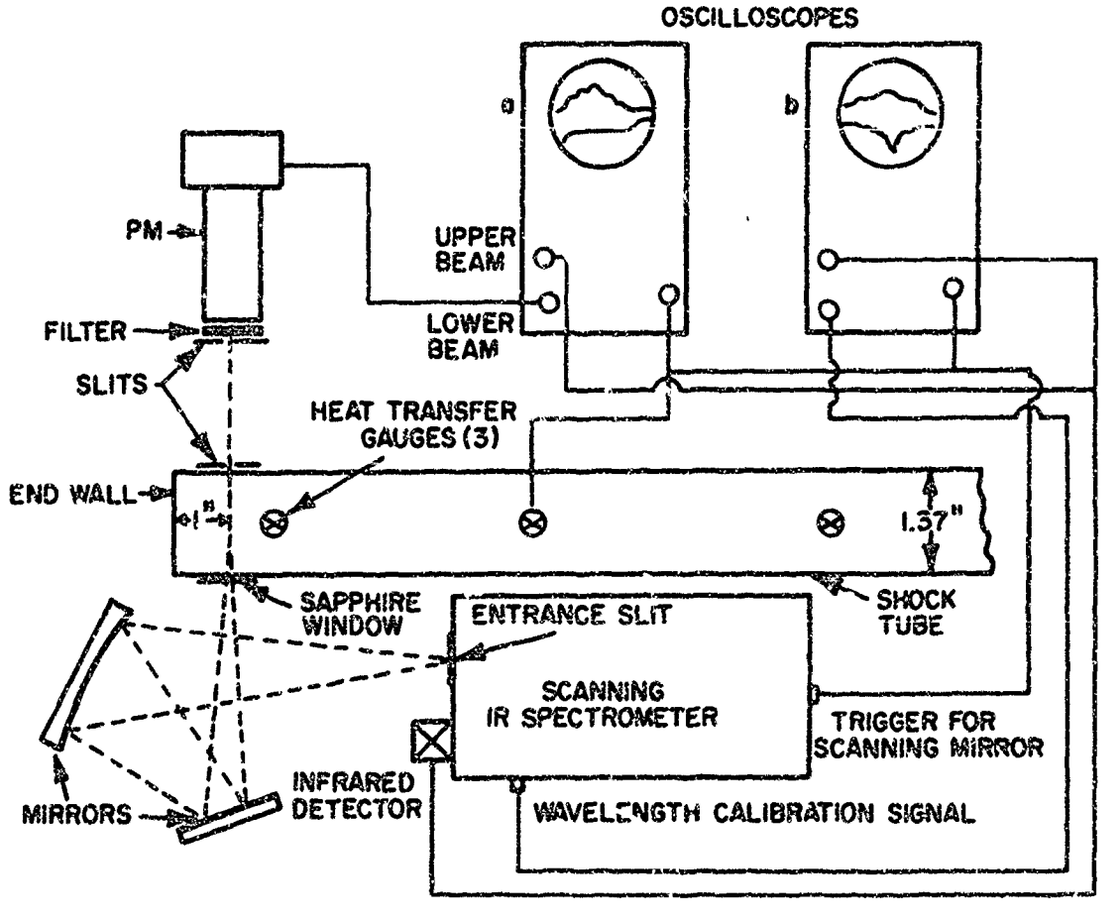

Fig. 15 Schematic of experimental arrangement of the scanning spectrometer in use on the shock tube.

shock velocity. On scope (a) the monitor photomultiplier and the infrared signal from the scanning spectrometer are displayed, while on scope (b) the IR signal and the wavelength calibration generator signal are displayed, generally at a different sweep speed than that of scope (a).

Figure 16 shows the oscillograms from a shock tube run which produces an equilibrium temperature of 9925°K in argon. The various traces represent the infrared signal from the spectrometer (1) and (3), the monitor photomultiplier (2), and the wavelength calibration signal (4). The time of shock arrival is indicated beneath the oscillogram of scope (a) and is seen to occur just prior to the initiation of the oscilloscope sweeps. The monitor signal is seen to rise for approximately 40 microseconds and then to remain constant for approximately 100 microseconds. This constant portion represents the equilibrium test gas and hence the test time. The contact surface between the shock gas and driver gas is seen to arrive at the test station at approximately 180 microseconds indicating the end of the available test time in this run. The wavelength scale shown on the oscillogram of scope (b) was obtained from the wavelength calibration signal. The infrared signal from the spectrometer under these conditions is primarily a continuum produced by the inelastic scattering of electrons by neutral species[46]. However, by means of this scanning technique contributions due to various known lines are also evident. A few of these lines have been indicated on the oscillogram at 2.42, 2.55 and 2.88 μ. These data can be reduced to an absolute spectral radiation intensity by applying the absolute calibration curve, Fig. 13, the vignette correction factor, Fig. 14, and a transmission correction for the sapphire window.

Figure 17 summarizes results obtained in shock heated argon at a temperature of 9900°K over the wavelength range of 2 - 5.4 μ. Each line segment was obtained from a single scan during a shock tube run from data such as is shown in Fig. 16. The data have been normalized to a standard temperature by using the monitor signal. The gaps in the spectral coverage are regions in which considerable structure due to lines occur. The regions have been removed in Fig. 17 in order to leave just the continuum contribution.

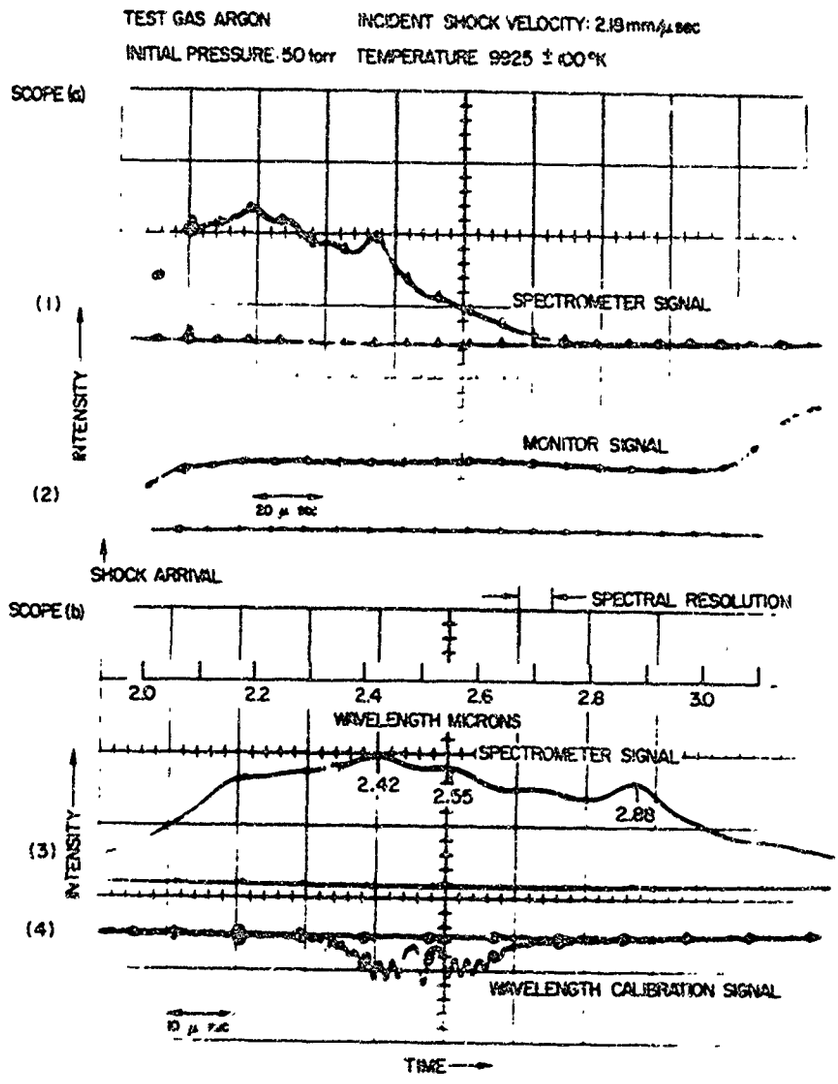

Fig. 16 Oscillogram showing data obtained with the scanning spectrometer from a shock tube experiment in argon producing an equilibrium temperature behind the reflected shock of 9925°K. Scope (a) shows signals from the scanning spectrometer (1) and the monitor photomultiplier (2) at a sweep speed of 20 μsec/cm. Scope (b) shows signals from the scanning spectrometer (3) and the wavelength calibration generator (4) at a sweep speed of 10 μsec/cm.

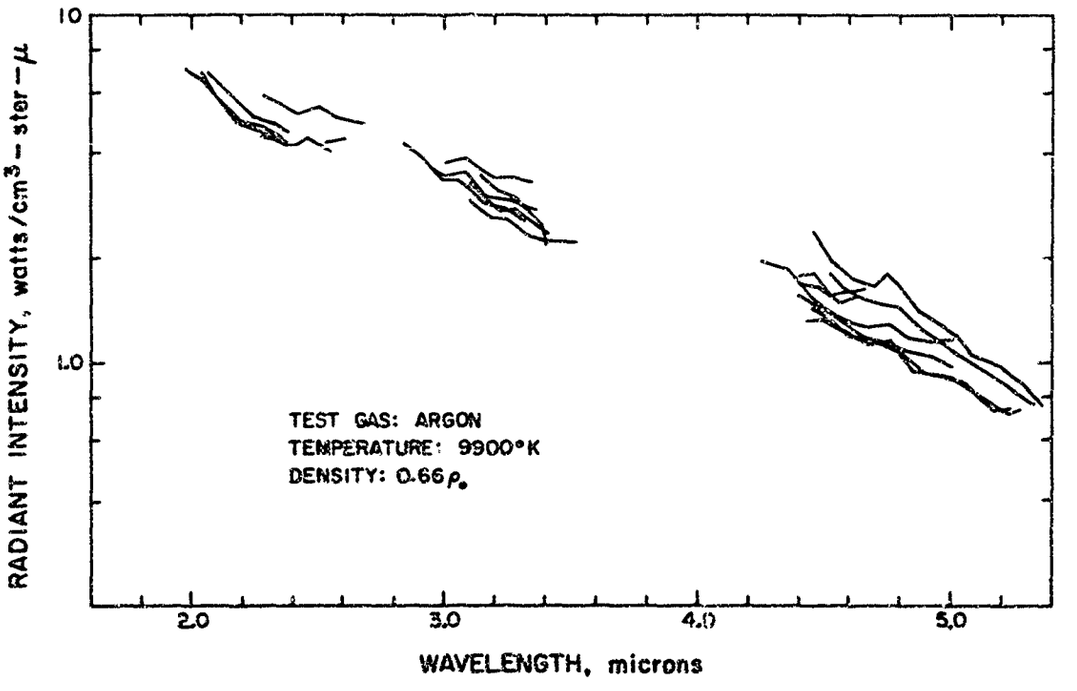

Fig. 17 Radiant intensity of continuum infrared radiation from argon shock heated to an equilibrium temperature of 9900°K as a function of wavelength. Each line represents a shock tube run using the scanning spectrometer. The gaps in the data are regions of line radiation which have been removed in this presentation to show just the continuum contribution.

Two obvious advantages of a scanning instrument are evident from these results: 1) by comparison to an earlier study made with a single channel spectrometer[46], it is obvious that far fewer runs with the scanning instrument are necessary to define a reasonable spectral region, and 2) scanning allows one to separate out continua from line and band radiators-which is an important consideration in studies devoted to obtaining absolute intensities of continuous sources. Of course, if it is the line or band contributions that are of interest, this instrument could also be used to separate the continuum radiation from discrete sources. For this purpose better spectral resolution than the current instrument might be desireable and could easily be obtained in the present design with a different grating at a sacrifice of a smaller spectral region scanned.

5. Summary

A synchronized high-speed scanning spectrometer has been described for operation in the infrared spectral region from 2 to 6 μ. Using a coarse grating with this instrument it is possible to scan 0.6μ to 30 μsec with spectral resolution of 0.07 μ. The scanning is achieved by spinning a small metallic mirror with a rapidly varying magnetic field. The mirror can be accelerated to constant angular velocity in about 15 μsec, which represents the minimum delay for synchronization with short duration source.

The instrument has been used to measure radiation intensities behind reflected shocks in various gases.* Under the studied conditions the radiation observed in these gases is primarily a continuum due to scattering of electrons from neutral species. The advantage of the use of a rapid scanning spectrometer for survey purposes and for absolute intensity measurements in shock tube work has been illustrated.

The instrument described in this report had rather low spectral resolution, since the radiation under study was primarily a continuum. However, as noted before, higher spectral resolution can be obtained by a simple change of grating and detectors but at the cost of a narrower spectral range per scan. The first version of this instrument was built

* The results of these studies will be published of a later date.

to scan from 1000 Å - 11,500 Å, with resolution of 50 Å.[45] A newer model has also been built which scans the region from 5000 Å - 12,000 Å. Several different gratings can be used and spectral resolution of 5 Å or better is possible. This newer instrument also incorporates an automatically resetting scanning mirror.

REFERENCES

1. Kivel, B., Mayer, H. and Bethe, H., "Radiation from Hot Air Part I - Theory of Nitric Oxide Absorption," Annals of Phys. 2, 57 (1957).

2. Keck, J., Camm, J., Kivel, B. and Wentink, T. Jr., "Radiation from Hot Air. Part II," Annals of Phy[illegible] (1959).

3. Kivel, B. and Bailey, K., "Tables of Radiation from [illegible] Temperature Air," Avco Everett Research Laboratory Research Report 21, December 1957.

4. Wentink, T. Jr., Planet, W., Hammerling, P. and Kivel, B., "Infrared Continuum Radiation from High Temperature Air," J. Appl. Phys. 29, 742 (1958).

5. Taylor, R. L., "Continuum Infrared Radiation from High Temperature Air and Nitrogen," J. Chem. Phys. 39, 2354 (1963).

6. Klein, M. M. and Brueckner, K. A., "Interaction of Slow Electrons with Atomic Oxygen and Atomic Nitrogen," Phys. Rev. 111, 1115 (1958).

7. Branscomb, Burch, Smith and Geltman, "Photodetachment Cross Section and the Electron Affinity of Atomic Oxygen," Phys. Rev. 111, 505 (1958).

8. Lin, S. C. and Kivel, B., "Slow-Electron Scattering by Atomic Oxygen," Phys. Rev., 114, 1026 (1959).

9. Alpher, R. A. and White, D. R., "Optical Refractivity of High-Temperature Gases I. Effects Resulting from Dissociation of Diatomic Gases," Phys. Fluids, 2, 153 (1959).

10. Neynaber, R. H., Marino, L. L., Rothe, E. W. and Trujillo, S. M., "Low-Energy Electron Scattering from Atomic Oxygen," Phys. Rev. 123, 148 (1961). Neynaber, R. H. Marino, L. L., Rothe, E. W. and Trujillo, S. M., "Low Energy Electron Scattering from Atomic Nitrogen," Phys. Rev. 129, 2069 (1963).

11. Chandrasekhar, S. and Breen, F. H., "On the Continuous Absorption Coefficient of the Negative Hydrogen Ion. III," Ap. J. 104, 430 (1946). Nedelsky, L., "Radiation from Slow Electrons," Phys. Rev. 42, 641 (1932).

12. Slater, J. C., Phys. Rev. 81, 385 (1951). Hammerling P., Shine, W.W. and Kivel, B., "Low-Energy Elastic Scattering of Electrons by Oxygen and Nitrogen," J. of App. Phys., 28, 760 (1957). Kivel, B., "Elastic Scattering of Low Energy Electrons by Argon," Phys. Rev. 116, 926 (1959).

13. Bates, D. R. and Massey, H.S.W., "The Negative Ions of Atomic and Molecular Oxygen," Phil. Trans. Roy. Soc. (London) A239, 269 (1943); "The Basic Reactions in the Upper Atmosphere II. The Theory of Recombination in the Ionized Layers," Proc. Roy. Soc. (London) A192, 1, (1947).

14. Hartree, Hartree and Swirles, "Self-Consistent Field, Including Exchange and Super-Position of Configurations, with Some Results for Oxygen," Phil. Trans. Roy. Soc. (London) A238, 229 (1939).

15. Hartree, D. R. and Hartree, W., "Self-Consistent Field, with Exchange, for Nitrogen and Sodium," Proc. Roy. Soc. (London) A193, 299 (1948).

16. Slater, J. C., "The Theory of Complex Spectra," Phys. Rev. 34, 1293 (1929).

17. Seaton, M. J., "The Hartree-Fock Equations for Continuous States with Applications to Electron Excitation of the Ground Configuration Terms of OI," Proc. Roy. Soc. (London) 245, 58 (1953).

18. Hundley, R. O., "Bremsstrahlung During the Collision of Low-Energy Electrons with Neutral Atoms and Molecules," The Rand Corporation, RM 3334-ARPA, October 1962.

19. Goldberger, M. L. and Watson, K. M., Collision Theory, John Wiley & Sons Inc., N. Y. (1964).

20. Stier, Von H. C., "Zur Deutung des Ramsaueréffektes bei symmetrischen, zweiato migen Molekulen," Zeitschrift fuer Physik 76:439-470 (1932).

21. Kivel, B., "Neutral Atom Bremsstrahlung," Avco Everett Research Laboratory Research Report 247, May 1966.

22. Nedelsky, L., "Radiation from Slow Electrons," Phys. Rev. 42, 641 (December 1, 1932).

23. Allis and Morse, "Theorie der Streuung langsamer Elektronen an Atomen," Zeits. f. Physik, 20, 567 (1931).

24 Ohmura, T. and Ohmura, H., "Continuous Absorption Due to Free-Free Transitions in Hydrogen," Phys. Rev. 121, 513 (1961), "Free-Free Absorption Coefficient of the Negative Hydrogen Ion," Astrophysical J., Vol. 131, (1960).

25. Geltman, S., "Continuum States of H^- and the Free-Free Absorption Coefficient," Ap. J. 141, 376 (1965).

26. Hundley, R. O., "Bremsstrahlung During the Collision of Low-Energy Electrons with Neutral Atoms and Molecules," The Rand Corporation, RM 3334-ARPA, October 1962.

27. Frost, L. S. and Phelps, A. V., "Rotational Excitation and Momentum Transfer Cross Sections for Electrons in H_2 and N_2 from Transport Coefficients," Phys. Rev. 127, 1621 (1962).

28. Hilsenrath, J. and Klein, J., "Tables of Thermodynamic Properties of Air in Chemical Equilibrium including Second Virial Corrections from 1500°K to 15,000°K," National Bureau of Standards, AEDC-TR-65-58 (March 1965).

29. Ramsauer, Von C. and Kollath, R., "Uber Den Wirkungsquerschnitt der Nichtedelgasmolekule Gegenuber Elektronen Unterhalb 1 Volt," Ann. d. Phys. 4, 91-108 (1930).

30. Allen, R. A., "Air Radiation Graphs: Spectrally Integrated Fluxes Including Line Contributions and Self Absorption," Avco Everett Research Laboratory Research Report 230 (Sept. 1965).

31. Gloersen, P., "Electronic-Recording, Time-Resolving Spectrometer", J. Opt. Soc. Am. 48, 712 (1958).

32. Bethke, G. W., "Ultrarapid-Scan Infrared Spectrometer", J. Opt. Soc. Am. 50, 1054 (1960).

33. Hill, R. A., and Beckner, E. H., "Rapid-Scan Spectrograph for Plasma Spectroscopy", J. Opt. Soc. Am. 54, 572 (1964).

34. Peacock, N. J., Cooper, J., and Greig, J. R., "Emission-line Profile Measurements in Transient Plasmas, using a Scanning Fabry-Perot Interferometer", Proc. Phys. Soc. 83, 803 (1964).

35. Dmitrievskii, O. D., "Super-Fast Photoelectric Spectrometer", Optics and Spect. 16, 547 (1964).

36. Dmitrievskii, O. D. and Kotlyar, I. P., "An Infrared Ultrafast Spectrometer", Optics and Spect. 19, 177 (1965).

37. Hill, R. A., "A Multiple-Scan, Rapid-Scan Spectrograph for Electron Density Measurements in Transient Plasmas", Appl. Opt. 4, 1593 (1965).

38. Herr, K. C., and Pimentel, G. C., "A Rapid-Scan Infrared Spectrometer; Flash Photolytic Detection of Chloroformic Acid and of CF_2, Appl. Opt. 4, 25 (1965).

39. Harber, R. A., and Sonnek, G. E., "Spectral Analysis using the Electronic Scanning Spectrometer", Appl. Opt. 5, 1039 (1966).

40. Hill, R. A., "Electron-Density Measurements in Transient Plasmas by Rapid-Scan Spectroscopy", Bull. Am. Phys. Soc., Series II, Vol. II, No. 4 (1966).

41. Church, C. H., and Gampel, L., "A Wide Spectral Range Ultra-Rapid Scan Spectrometer", Appl. Opt. 5, 241 (1966).

42. Hand, C. W., Kaufmann, P. Z., and Hexter, R. M., "Kinetic Spectroscopy in the Infrared: a Rapid-Scan Infrared Spectrometer", Appl. Opt. 5, 1097 (1966).

43. Hill, R. A., and Fellerhoff, R. D., "A Dual Recording, Variable Range, Rapid-Scan Spectrometer; Comparison of Simultaneously Recorded Stark-Broadened Hα and Hβ Line Profiles", Appl. Opt. 5, 1105 (1966).

44. Camm, J. C., "A Synchronized High Speed Scanning Spectrometer," Avco Everett Research Laboratory Research Note 447, February 1965.

45. Conn, G. K. T., "Optical Theory of the Echelette Grating," Camb. Phil. Soc. Proc., 43, 240 (1947).

46. Taylor, R. L., "Continuum Infrared Radiation from High Temperature Air and Nitrogen", J. Chem. Phys. 39, 2354 (1963).

UNCLASSIFIED

Security Classification

DOCUMENT CONTROL DATA - R&D

(Security classification of title, body of abstract and indexing annotation must be entered when the overall report is classified)

1. ORIGINATING ACTIVITY (Corporate author) AVCO Everett Research Laboratory 2385 Revere Beach Parkway Everett, Massachusetts 02149	2a. REPORT SECURITY CLASSIFICATION UNCLASSIFIED 2b GROUP

3. REPORT TITLE

OPACITY OF LOW-TEMPERATURE AIR

4. DESCRIPTIVE NOTES (Type of report and inclusive dates)

1 September 1965-1 September 1966

5. AUTHOR(S) (Last name, first name, initial)

Camm, J. C.; Kivel, B.; Taylor, R. L.; et al.

6. REPORT DATE	7a. TOTAL NO. OF PAGES	7b. NO. OF REFS
March 1967	96	46

8a CONTRACT OR GRANT NO. AF 29(601)-7055 b. PROJECT NO. 5710 c. Subtask No. 07.003 d	9a. ORIGINATOR'S REPORT NUMBER(S) AFWL-TR-66-127 9b. OTHER REPORT NO(S) (Any other numbers that may be assigned this report) October 1966 Contractor report No. AERL Final Report-

10. AVAILABILITY/LIMITATION NOTICES This document is subject to special export controls and each transmittal to foreign governments or foreign nationals may be made only with prior approval of AFWL (WLRT), Kirtland AFB, NM, 87117. Distribution is limited because of the technology discussed in the report.

11. SUPPLEMENTARY NOTES	12. SPONSORING MILITARY ACTIVITY
	AFWL (WLRT) Kirtland AFB, NM 87117

13. ABSTRACT Predictions are given for the Bremsstrahlung absorption cross section of atomic oxygen and atomic nitrogen. The electron-atom interaction potential energy is adjusted to give agreement with the photo-absorption measurements of the negative oxygen ion. The exchange force is treated in an approximate manner following a suggestion by Slater but adjusted to take account of the dependence on the configuration of the electron wave. The difference in the exchange force for s- and p-waves as well as the difference between the triplet and quintet configurations in atomic nitrogen must be preserved to obtain predictions for the Bremsstrahlung which are in agreement with experiments. The partial wave analysis for Bremsstrahlung and elastic scattering by molecular nitrogen is reviewed. These studies suggest that the Bremsstrahlung in the field of molecular nitrogen can be estimated from the measured momentum transfer cross section. Using this approximation for the molecular components and recent calculations of Bremsstrahlung in the field of atomic oxygen and nitrogen, the emissivity and intensity from neutral Bremsstrahlung in high-temperature air is estimated. A spectrometer which scans a wavelength band of 0.6 microns in 30 microseconds and is useful from 2 to 6 microns is described. Using this instrument, data have been obtained of the absolute spectral radiation intensity of air, nitrogen, neon, and argon heated by reflected shocks in shock tubes to equilibrium temperatures in the range of 6000 to 10,000°K. In this temperature regime, an important source of continuum radiation in these gases is neutral Bremsstrahlung caused by the inelastic scattering of electrons from neutral atoms and molecules.

(Distribution Limitation Statement No. 2)

DD FORM 1 JAN 64 1473

UNCLASSIFIED

Security Classification

14. KEY WORDS	LINK A		LINK B		LINK C	
	ROLE	WT	ROLE	WT	ROLE	WT
Bremsstrahlung						
Neutral molecule Bremsstrahlung						
Neutral atom Bremsstrahlung						
High-temperature air						
Elastic scattering of atomic oxygen and nitrogen						
Air radiation						
Exchange force in electron scattering						
Infrared radiation						
Spectroscopy						
Spectrometer						
Rapid scanning						
Shock tube						

INSTRUCTIONS

1. ORIGINATING ACTIVITY: Enter the name and address of the contractor, subcontractor, grantee, Department of Defense activity or other organization *(corporate author)* issuing the report.

2a. REPORT SECURITY CLASSIFICATION: Enter the overall security classification of the report. Indicate whether "Restricted Data" is included. Marking is to be in accordance with appropriate security regulations.

2b. GROUP: Automatic downgrading is specified in DoD Directive 5200.10 and Armed Forces Industrial Manual. Enter the group number. Also, when applicable, show that optional markings have been used for Group 3 and Group 4 as authorized.

3. REPORT TITLE: Enter the complete report title in all capital letters. Titles in all cases should be unclassified. If a meaningful title cannot be selected without classification, show title classification in all capitals in parenthesis immediately following the title.

4. DESCRIPTIVE NOTES: If appropriate, enter the type of report, e.g., interim, progress, summary, annual, or final. Give the inclusive dates when a specific reporting period is covered.

5. AUTHOR(S): Enter the name(s) of author(s) as shown on or in the report. Enter last name, first name, middle initial. If military, show rank and branch of service. The name of the principal author is an absolute minimum requirement.

6. REPORT DATE: Enter the date of the report as day, month, year; or month, year. If more than one date appears on the report, use date of publication.

7a. TOTAL NUMBER OF PAGES: The total page count should follow normal pagination procedures, i.e., enter the number of pages containing information.

7b. NUMBER OF REFERENCES: Enter the total number of references cited in the report.

8a. CONTRACT OR GRANT NUMBER: If appropriate, enter the applicable number of the contract or grant under which the report was written.

8b, 8c, & 8d. PROJECT NUMBER: Enter the appropriate military department identification, such as project number, subproject number, system numbers, task number, etc.

9a. ORIGINATOR'S REPORT NUMBER(S): Enter the official report number by which the document will be identified and controlled by the originating activity. This number must be unique to this report.

9b. OTHER REPORT NUMBER(S): If the report has been assigned any other report numbers *(either by the originator or by the sponsor)*, also enter this number(s).

10. AVAILABILITY/LIMITATION NOTICES: Enter any limitations on further dissemination of the report, other than those imposed by security classification, using standard statements such as:

(1) "Qualified requesters may obtain copies of this report from DDC."

(2) "Foreign announcement and dissemination of this report by DDC is not authorized."

(3) "U. S. Government agencies may obtain copies of this report directly from DDC. Other qualified DDC users shall request through _____."

(4) "U. S. military agencies may obtain copies of this report directly from DDC. Other qualified users shall request through _____."

(5) "All distribution of this report is controlled. Qualified DDC users shall request through _____."

If the report has been furnished to the Office of Technical Services, Department of Commerce, for sale to the public, indicate this fact and enter the price, if known.

11. SUPPLEMENTARY NOTES: Use for additional explanatory notes.

12. SPONSORING MILITARY ACTIVITY: Enter the name of the departmental project office or laboratory sponsoring *(paying for)* the research and development. Include address.

13. ABSTRACT: Enter an abstract giving a brief and factual summary of the document indicative of the report, even though it may also appear elsewhere in the body of the technical report. If additional space is required, a continuation sheet shall be attached.

It is highly desirable that the abstract of classified reports be unclassified. Each paragraph of the abstract shall end with an indication of the military security classification of the information in the paragraph, represented as *(TS)*, *(S)*, *(C)*, or *(U)*.

There is no limitation on the length of the abstract. However, the suggested length is from 150 to 225 words.

14. KEY WORDS: Key words are technically meaningful terms or short phrases that characterize a report and may be used as index entries for cataloging the report. Key words must be selected so that no security classification is required. Identifiers, such as equipment model designation, trade name, military project code name, geographic location, may be used as key words but will be followed by an indication of technical context. The assignment of links, rules, and weights is optional.